## TRMM and Other Data Precipitation Data Set Documentation

George J. Huffman (1) David T. Bolvin (1,2)

(1) Mesoscale Atmospheric Processes Laboratory, NASA Goddard Space Flight Center (2) Science Systems and Applications, Inc.

26 April 2018

### "Recent" News

- 26 April 2018 DOI's have been assigned for 3B42 and 3B43.
- 23 December 2016 Anomalies in the DMSP F-16 input data for the TMPA-RT created streaks of precipitation over open-ocean regions. The faulty data input data were deleted and TMPA-RT was rerun for the period 18 December 2016 at 09 UTC to 19 December 2016 at 18 UTC.
- 27 September 2016 A user discovered that the January 2016 IMERG Final Run lacked gauge data, which turned out to stem from a failed change of code to accommodate a change in format for the GPCC gauge analysis. This also affected the TMPA production, and forced the re-run of January-June 2016.
- 10 May 2016 The data flow from the Himawari-8 GEO satellite was interrupted for 57 hours, 7 May, 05 UTC 9 May, 14 UTC and during that time there are patches of missing values in the merged precipitation data, and continuous zones of missing values in the IR precipitation data in the center of the Himawari-8 sector (over Japan), where data from the adjoining satellites are unable to fill the gap.
- 7 July 2015 MTSat-2 was replaced by Himawari 8 effective 02 UTC on 7 July 2015.
- 8 April 2015 TMI data are no longer input to the products because they were terminated on 8 April 2015 as part of the TRMM satellite end-of-mission activities.
- 11 February 2015 The 3B42/43 system was restarted for October 2014 using a climatological calibration in place of the routine TCI-TMI calibration, due to the termination of routine PR-based products on 8 October 2014.
- 25 May 2014 Metop-A was restored to functionality; the date were again available starting 0746 UTC 21 May 2014.
- 28 March 2014 Metop-A had an apparent hardware failure at 1400 UTC on 27 March 2014 and the instrument is off.
- 15 February 2014 Snow accumulation on the receiving antenna prevented reception of MTSAT-2 data from 1832 UTC on 14 February 2014 to 1232 UTC on 15 February 2014. The data are lost.
- 12 November 2013 A TRMM spacecraft anomaly resulted in the loss of most TRMM sensor data for the period 02-14 UTC on 12 November 2013, and additional issues resulted in data gaps during the period 20-23:30 UTC. This reduces the data content in 3B42/43 somewhat, but is not a serious issue overall.

16 August 2013 Metop-B was added as an input data source on 15 August 2013; the first use in 3B42/43 is the July 2013 processing.

28 January 2013 Processing issues were discovered with both the Version 7 TMPA production (3B42/43) and Version 7 TMPA-RT (3B40/41/42RT) data series and it was decided to re-do the retrospective processings to correct the issues. In general the original Version 7 data sets are considered an improvement over Version 6, but this additional processing is considered important to meet the goals of the project. Users are urged to switch to the newest Version 7 data sets as soon as practical. See "additional processing for Version 7" for more details.

25 September 2012 GOES-E (GOES-13) developed problems with the sounder and some IR channels starting 20 September 2012. Eventually it was placed in safe mode and subsequently GOES-15 was programmed to take over GOES-E observational schedule. Data are affected in the GOES-E sector, roughly the Americas. Recovery efforts for GOES-13 are on-going.

Visual inspection of the 3B41RT data shows some missing data during the period 23 September 22 UTC through 24 September 10 UTC. Even when the data in the GOES-E sector aren't missing, the alternative satellites used to provide the fill-in by NOAA/CPC don't necessarily exhibit the same bias characteristics from satellite to satellite, probably due to the use of data at a variety of zenith angles. Visual evidence of bias differences due to fill-in data starts at the same time, 23 September 22 UTC, and extends through 24 September 17 UTC.

19 June 2012 The current satellite-gauge combination scheme allows coastal gauge data to "bleed" into coastal waters, up to 1° away from the coast. This is particularly noticeable where there is heavy precipitation in the gauge analysis, but modest values off-shore. As well, GOES-E data in the GridSat-B1 archive is highly noisy for 9-15 UTC 5 March 1998, 00Z March 25, and 21Z March 29, effectively preventing useful estimates over the Americas for IR precipitation and precipitation. It is suggested to use HQ precipitation instead.

22 May 2012 Version 7 of TRMM products 3B42 and 3B43 has now been implemented, which supersedes all previous versions, including the recent Versions 6 and 6a (ended on 30 June 2011). For more details, see "Transition from Version 6 to Version 7" in the technical documentation (available as ftp://precip.gsfc.nasa.gov/pub/trmmdocs/3B42 3B43 doc.pdf).

#### Contents

- 1. Data Set Names and General Content
- 2. Related Projects, Data Networks, and Data Sets
- 3. Storage and Distribution Media
- 4. Reading the Data
- 5. Definitions and Defining Algorithms
- 6. Temporal and Spatial Coverage and Resolution
- 7. Production and Updates
- 8. Sensors
- 9. Error Detection and Correction
- 10. Missing Value Estimation and Codes
- 11. Quality and Confidence Estimates

- 12. Data Archives
- 13 Documentation
- 14. Inventories
- 15. How to Order and Obtain Information about the Data

# **Keywords** (searchable as \*keyword\*)

**IMERG** 

2A12 intercomparison results

2B31

3B42 IR data correction 3B42 data fields known anomalies

3B42RT known data set access issues

3B43 known errors

3B43 data fields Merged 4-Km IR Tb data set

accuracy MHS

additional processing for Version 7 MHS precipitation data set ambiguous pixels MHS error detection/correction

AMSR-E missing hours AMSR-E error detection/correction obtaining data

period of record AMSU-B

AMSU-B precipitation data set PR

AMSU-B error detection/correction PR error detection/correction archive and distribution sites precipitation gauge analysis

controlling factors on dataset performance

precipitation phase data access policy

precipitation variable data file access technique production and updates

random error data file layout data providers relativeError

data set archive rain gauge analysis (see "precipitation gauge

analysis") data set creators data set inventory read a file of data data set name references

diurnal cycle sensors contributing to TMPA

documentation creator SG combination

documentation revision history similar data sets DOIs for 3B42 and 3B43 spatial coverage estimate missing values spatial resolution

file date **SSMI** 

Frequently Asked Questions (FAQ) SSMI error detection/correction Giovanni SSMI Level 2 precipitation estimates

**GPROF** 

grid SSMIS error detection/correction GridSat-B1 IR Tb data set SSMIS Level 2 precipitation estimates

standard missing value HQ+VAR temporal resolution

time zone TMI TMI error detection/correction transition from Version 6 to Version 7 TRMM
TRMM end of mission issues
units of the TMPA estimates
VAR

### 1. Data Set Names and General Content

The formal \*data set name\* is the "TRMM and Other Data Precipitation Data Set." The algorithm applied is the Version 7 TRMM Multi-Satellite Precipitation Analysis. For convenience, the data set is referred to in this document as the "TMPA." Note that there are other products in the general TRMM data inventory, so it is important to be specific about the product being used.

The data set currently contains two products, three-hourly combined microwave-IR estimates (with gauge adjustment) and monthly combined microwave-IR-gauge estimates of precipitation computed on quasi-global grids about two months after the end of each month starting in January 1998.

Huffman et al. (2007, 2010) are the primary refereed citations for the TMPA, while this documentation is the primary source of current technical information. Huffman et al. (2003, 2005) provide earlier short formal summaries.

.....

## 2. Related Projects, Data Networks, and Data Sets

The \*data set creators\* are G.J. Huffman, D.T. Bolvin, E.J. Nelkin, and R.F. Adler, working in the Mesoscale Atmospheric Processes Laboratory, NASA Goddard Space Flight Center, Code 612, Greenbelt, Maryland, and E.F. Stocker, working in the Precipitation Processing System (PPS, formerly the TRMM Science Data and Information System), NASA Goddard Space Flight Center, Code 610.2, Greenbelt, Maryland.

.....

The work is being carried out as part of the Tropical Rainfall Measuring Mission (\*TRMM\*), an international project of NASA and JAXA designed to provide improved estimates of precipitation in the Tropics, where the bulk of the Earth's rainfall occurs. TRMM began recording data in December 1997 and ended in April 2015. It flew in a (46-day) precessing orbit at a 35° inclination with a period of about 91.5 min. This orbit allows TRMM to build up a complete view of the climatological diurnal cycle, as well as providing calibration for other precipitation-relevant sensors in Sun-synchronous orbits. The TRMM home page is located at <a href="http://trmm.gsfc.nasa.gov/">http://trmm.gsfc.nasa.gov/</a>.

.....

The TMPA draws on data from several \*data providers\*:

1. NASA/GSFC Level 1 TMI Tb's (processed with TRMM algorithm 2A12 at PPS);

- 2. NASA/GSFC Level 2 PR-TMI "tall vector" precipitation estimates (processed with TRMM algorithm 2B31 at PPS);
- 3. NSIDC Level 2 AMSR-E precipitation estimates (processed with GPROF2004-AMSR at MSFC/GHRC);
- 4. NOAA/NCDC CLASS SSMI Tb's (processed with GPROF2010-SSMI at CSU);
- 5. NOAA/NCDC CLASS SSMIS Ta's (processed with GPROF2004v-SSMIS at PPS);
- 6. NESDIS/MSPPS operational Level 2 (NOAA-series) AMSU-B precipitation estimates;
- 7. NESDIS/MSPPS operational Level 2 (NOAA- and MetOp-series) MHS precipitation estimates;
- 8. NOAA/NCDC Level 3 GridSat-B1 IR Tb Data (processed into VAR at PPS);
- 9. NOAA/NWS/CPC Level 3 Merged 4-Km Geostationary Satellite IR Brightness Temperature Data (processed into VAR at PPS as part of the TMPA); and
- 10. GPCC Level 3 Full and Monitoring Precipitation Gauge Analyses.

See "sensors contributing to TMPA" for more details.

Some of these data sets extend beyond the TMPA period in their original archival location	lS.
---	-----

.....

There are numerous \*similar data sets\*, although no other quite matches all the attributes of being routinely produced, publicly available, fine-scale in space and time, quasi-global, available from January 1998 onwards, intercalibrated, and formed by combining multiple data sources including precipitation gauges. The International Precipitation Working Group data set tables at http://www.isac.cnr.it/~ipwg/data/datasets.html provide a good listing of other precipitation data sets. The closest include the set of estimates based on:

- 1. the previous Version 6 TMPA estimates;
- 2. Turk (1999): individual SSMI overpasses calibrate geo-IR precipitation estimates;
- 3. Sorooshian et al. (2000): the PERSIANN neural network calibrates IR with microwave;
- 4. Joyce et al. (2004): the CMORPH morphing scheme time-interpolates microwave patterns with IR-based motion vectors; and
- 5. Kubota et al. (2007): the GSMaP system applies a Lagrangian time-interpolation scheme similar to CMORPH.
- 6. Huffman et al. (2017), the IMERG data sets, which are the successor to TMPA and TMPA-RT, and will supersede them when retrospectively processed for the TRMM era in Fall 2018.

Several SSMI/SSMIS-based data sets are available as gridded single-sensor data sets with significant data voids in cold-land, snow-covered, and ice-covered areas, including those computed with the GPROF 6.0, 2004a, and 2010 algorithms (based on Kummerow et al. 1996); the NOAA Scattering algorithm (Grody 1991); and the Chang/Chiu/Wilheit emission algorithm (Wilheit et al. 1991, Chiu and Chokngamwong 2010) among others. Other daily, single-sensor data sets are available for open-water regions based on SSMI/SSMIS data (RSS, Wentz and Spencer 1998; HOAPS, Andersson et al. 2010), MSU data (Spencer 1993), AMSR-E, and AMSU-B/MHS data. Several daily single-sensor or combination data sets are available at the regional scale, but are not really "similar."

The Real-Time TMPA product (3B42RT) is being computed with the TMPA-RT in near-real time, and constitutes the most timely source of TMPA estimates. See "3B42RT" for details.

.....

The Version 7 Real-Time TRMM product \*3B42RT\* (not to be confused with the Version 7 production TRMM product 3B42) is being computed with the TMPA in near-real time, and constitutes the most timely source of TMPA estimates. The near-real time computation requires several simplifications in 3B42RT compared to 3B42:

- 1. The complete 3B42RT data record is not reprocessed as upgrades are made to the procedure its main focus is timeliness.
- 2. The IR calibration period is a trailing approximately 30-day accumulation, rather than the calendar month in which the observation time falls.
- 3. A real-time version of the GPROF-TMI is used as the calibrating standard because the TRMM Combined Instrument product (2B31) is not available in real time.
- 4. In near-real time it is not possible to apply precipitation gauge data. Rather, a climatological correction to the Version 7 production 3B42 is applied that varies by month and location to approximately account for the different calibrators and the use of precipitation gauge data in 3B42.

Note that 3B42 estimates are considered to supersede the 3B42RT estimates as each month of 3B42 is computed. The 3B42 processing is designed to maximize data quality, so 3B42 is strongly recommended for any research work not specifically focused on real-time applications.

The first set of retrospectively processed data for Version 7 3B42RT was released in June 2012 using the Version 7 3B42 for calibration, while the second set were posted in December 2012 (see "additional processing for Version 7"). This version includes the following:

- 1. SSMIS data are introduced based on interim calibration developed in conjunction with D. Vila (ESSIC).
- 2. The RT system is retrospectively processed back to 1 March 2000 using the full satellite data sets available in the Version 7 production system. The main difference from true RT processing is that the production data records are somewhat more complete than those available in real time. The start date is driven by the start date of the CPC Merged 4 Km IR data record. It continues to be the case that, despite the long RT record, it is strongly recommended that the production dataset (3B42) be used for all research not specifically focused on RT applications.
- 3. Upon this release RT data that pre-date Version 6 continue to be provided in subdirectory *old*, while Version 6 RT data are moved to subdirectory *V06*.

See ftp://meso-a.gsfc.nasa.gov/pub/trmmdocs/rt/3B4XRT doc.pdf for more details.

It is planned that both the production and RT TMPA systems will be superseded by Integrated Multi-satellitE Retrievals for GPM (IMERG), although they will continue to be computed until IMERG is considered mature, first in early 2017 for the GPM era and Fall 2018 for the entire TRMM/GPM era. See the section on IMERG for more details.

.....

The \*transition from Version 6 to Version 7\* for TRMM datasets occurred on 30 June 2011, with June 2011 being the final month of Version 6 data. Thereafter, the Precipitation Processing System (PPS) was reconfigured to start the parallel activities of Version 7 "initial processing" (IP) for new data (starting 1 July 2011), and Version 7 reprocessing (RP) for the entire archive starting 1 January 1998. The TMPA lagged the other TRMM products to allow for calibration and to finalize use of SSMIS data. This release incorporated several important changes as part of the upgrade to Version 7:

- Additional satellites, including the early parts of the MHS record, the entire operational SSMIS record, and slots for future satellites.
- A new IR brightness temperature dataset for the period before the start of the CPC 4-km Merged Global IR Dataset (i.e., January 1998 February 2000). Unlike the old GPCP histograms used in Version 6, the NCDC GridSat-B1 features spatial resolution finer than the TMPA 0.25 grid and full coverage of the TMPA domain.
- Uniformly reprocessed input data using current algorithms, most notably for AMSU and MHS, but also including TCI, TMI, AMSR-E, and SSMI.
- Use of a single, uniformly processed surface precipitation gauge analysis using current algorithms as computed by the Global Precipitation Climatology Centre (GPCC).
- Use of a latitude-band calibration scheme for all satellites (see "HQ").
- Additional output fields in the data files, including sensor-specific source and overpass time.

The complete Version 6 archive was maintained for public access throughout and beyond the cutover to Version 7. Residual issues with satellite intercalibration, particularly for the early IR data and the SSMIS precipitation estimates, are currently being worked for the TMPA. For Initial Processing (IP), our switch to the GPCC gauge analysis necessitates increasing the latency of the products from 10 days after the month, which was the case in Version 6, to about two months after the end of the month. The initial Version 7 release occurred in May 2012, while the second set was posted in December 2012. See "additional processing for Version 7" for more details.

Initial testing shows that the revisions have eliminated the unrepresentatively low bias in ocean values for 2001-2007 that were related to how we treated an early version of AMSU-based precipitation. However, we find that the V7 tropical-ocean average precipitation is consistently some 5% higher than the combined TMI-PR product (2B31) that serves as the calibrator. The basis for this difference is not explicated at this point, but the value is small enough and consistent enough that we are choosing to release the data as background work continues. See "intercomparison results" for more details.

.....

An \*additional processing for Version 7\* was carried out when processing issues were discovered with both the Version 7 TMPA production (3B42/43) and Version 7 TMPA-RT (3B40/41/42RT) data series. In general, the original Version 7 data sets are considered an improvement over Version 6, but this additional processing is considered important to meet the goals of the project. Users are urged to switch to the newest Version 7 data sets as soon as practical.

In November 2012 it was discovered that AMSU and data were omitted in the first retrospective processing of both the Version 7 TMPA (3B42/43) and TMPA-RT (3B40/41/42RT) data series, which created an important shortcoming in the inventory of microwave precipitation estimates used during 2000-2010. In addition, a coding error in the TMPA-RT replaced the occasional missing-filled areas in product 3B42RT with zero-fills. Accordingly, both product series were retrospectively processed again. The main impact in both series was to improve the fine-scale patterns of precipitation during the periods noted below, roughly 2000-2010 (3B42/43) and 2000-2012 (3B4xRT). Averages over progressively larger time/space scales should be progressively less affected. [This is the reason the lack of AMSU went undiscovered; the merger system copes very reasonably with missing data.] Nonetheless, users were urged to switch to the newest Version 7 data sets as soon as practical. Subsequently, Yong et al. (2015) pointed out that F16 SSMIS data were also missing in the first retrospective processing.

It should be noted that these retrospective processings were done with archived "production" input data. For the RT, this resulted in some instances in which files that originally had not been received in a timely fashion, and hence did not make it into the original RT product, were ultimately archived when they showed up later, and then were included in the new retrospective processing. As such, the retrospectively processed RT is built from a superset of the data that had actually been available in true real time. The main implication is that the current "Initial Processing" RT being run only on real-time input could have somewhat worse errors than the equivalent reprocessed data.

In the original archive sites the newest runs may be identified by the file name suffixes. Specifically:

- V.7 3B42/43: "7A.HDF" for January 2000 September 2010 on http://mirador.gsfc.nasa.gov/cgi/bin/mirador/presentNavigation.pl?tree=project&project=T RMM&dataGroup=Gridded;
- V.7 3B4xRT: suffix of "7R2.bin" for 00 UTC 1 March 2000 05 UTC 7 November 2012 on ftp://trmmopen.gsfc.nasa.gov/pub/merged/mergeIRMicro/.

However, the secondary archive at ftp://disc2.nascom.nasa.gov/data/TRMM/Gridded/ associated with Giovanni currently requires a uniform naming convention for each data series. Thus, users must inspect the file date/times to determine that the data are the latest:

- V.7 3B42/43: original retrospectively processed data were posted in late May 2012, the newly reprocessed data (for January 2000 September 2010) were posted in December 2012, and Initial Processing data were posted as produced.
- V.7 3B4xRT: newly reprocessed data (for 00 UTC 1 March 2000 05 UTC 7 November 2012) were posted in January 2013, then Initial Processing data were posted as produced.

In the second retrospective processing it continues to be the case that the Version 7 3B42/43 is some 5-8% higher than the calibrating data set (2B31) over oceans, which is believed to be erroneous. However, the first several attempts at diagnosing this issue have not been fruitful. At the large scales this offset seems to be nearly a proportional constant. Another known issue is that RT over land seems to have an increasing trend that is strongest in south-central Asia and northwestern South America, again for reasons we do not yet understand. The RT trend over land is somewhat weaker in the second retrospective processing.

.....

## 3. Storage and Distribution Media

The official \*data set archive\* consists of Hierarchical Data Files (HDF). Each 3-hour dataset (3B42) or monthly dataset (3B43) is contained in a separate file with standard self-documenting HDF metadata. The 3B42/3B43 data are distributed via the Internet. Each 3B42 file is approximately 11 MB (uncompressed), while the 3B43 files are each 5 MB (uncompressed). See "DOIs for 3B42 and 3B43" for DOI information.

The full collection of 3B42/3B43 files are provided and archived by PPS at <a href="https://pmm.nasa.gov/data-access/pps-ftp#arthurhou-trmmdata/">https://pmm.nasa.gov/data-access/pps-ftp#arthurhou-trmmdata/</a>. and other locations indexed at <a href="https://pmm.nasa.gov/data-access/downloads/trmm">https://pmm.nasa.gov/data-access/downloads/trmm</a>. Other independent sources of these data files exist, but it is incumbent on the users to ensure that the data are the latest version and have a documented provenance.

Web-based interactive access to the 3B42/43 and related data is provided through Giovanni; see that topic for details.

.....

- 1. Besides the primary data sites (see \*data set archive\*), several "mirror" and value-added archive sites include the TMPA data sets and/or value-added products in their holdings. Users availing themselves of these sites should work with the personnel in charge of those sites to work out access problems. Also, users are urged to gain a clear understanding of the provenance of those data to assure that they are working with current, clean data.
- 2. FTP access is sometimes regulated by the ISP or institution providing Internet connectivity. Specifically, many ISP's and institutions only permit the FTP software on user machines ("clients") to make "passive" FTP connections. At least some Macintosh and Windows native FTP applications default to "active". Users having trouble with FTP access should consult with their computer system support personnel to determine whether this is an issue, and if so, whether shifting to a third-party FTP package is necessary to allow "passive" operation.
- 3. The TMPA data sets are in IEEE "big-endian" floating-point format. Generally Intel-based computers run in "little-endian", meaning the data must be "byte-swapped" to be useful.

.....

\*Giovanni\*, formerly the Geospatial Interactive Online Visualization ANd aNalysis Infrastructure, is created and supported by GES DISC. It provides a web-based resource for accessing many Earth science data sets, including IMERG Runs. It performs a variety of basic subsetting, time- and space-averaging, and output of results in plots, time series, animations, or ASCII text. The current Version 4 of Giovanni is located at

https://giovanni.sci.gsfc.nasa.gov/giovanni/.

## 4. Reading the Data

<sup>\*</sup>Known data set access issues\* include:

The \*data file layout\* and \*data file access technique\* details are provided for 3B42 at http://disc.gsfc.nasa.gov/precipitation/TRMM\_README/TRMM\_3B42\_readme.shtml and for 3B43 at http://disc.gsfc.nasa.gov/precipitation/TRMM\_README/TRMM\_3B43\_readme.shtml. The file specification can be accessed at http://pps.gsfc.nasa.gov/ppsdocuments.html#7guide.

.....

It is possible to \*read a file of data\* with many standard data-display tools. Any tool that reads the standard HDF file can be used to process 3B42 and 3B43 files. For example, the GDISC has developed procedures to import both TRMM HDF and binary data into ENVI. Links to them are posted as part of <a href="http://disc.sci.gsfc.nasa.gov/additional/faq/precipitation\_faq.shtml">http://disc.sci.gsfc.nasa.gov/additional/faq/precipitation\_faq.shtml</a>. As well, PPS provides a toolkit with C and FORTRAN versions that allow users to write custom programs. See <a href="http://pps.gsfc.nasa.gov/tsdis/Documents/ICSVol4.pdf">http://pps.gsfc.nasa.gov/tsdis/Documents/ICSVol4.pdf</a> for more details, although it lacks mention of the data fields that are new to Version 7.

.....

## 5. Definitions and Defining Algorithms

The \*precipitation variable\* is computed as described under the individual product headings. All precipitation products have been converted from their original units to mm/h. Throughout this document, "precipitation" refers to all forms of precipitation, including rain, drizzle, snow, graupel, and hail (see \*precipitation phase\*).

.....

The \*precipitation phase\* is not explicitly treated by the TMPA or its input datasets. The algorithms sense total hydrometeor mass in the atmospheric column (except the passive microwave retrievals only consider total solid hydrometeor mass over land and coast. Also, note that the passive microwave algorithms cannot retrieve any precipitation over a snowy/icy surface, regardless of the phase of the surface precipitation, although it is generally snow. The IR retrievals are calibrated to the passive microwave retrievals, again, without reference to precipitation phase. These IR calibrations are in-filled from surrounding areas in the snowy/icy-surface areas where microwave cannot provide estimates. Given these facts, the "precipitation" reported in this document refers to all forms of precipitation, including rain, drizzle, snow, graupel, and hail.

The \*time zone\* for this data set is Universal Coordinated Time (UTC, also as GMT or Z).

Because the data are provided at nominal UTC hours, each 3B42 data set represents a nominal +/-90-minute span around the nominal hour. Thus, the 00 UTC images include data from the very end of the previous UTC day.

.....

The \*GridSat-B1 IR Tb data set\* is produced by the NOAA National Climatic Data Center (NOAA/NCDC) under the direction of K Knapp, located in Asheville. The International Satellite Cloud Climatology Project (ISCCP) archived the "B1" subset of the full resolution

geostationary data subsampled (not interpolated) to ~10-km resolution at 3-hourly intervals beginning in 1983 from each cooperating geostationary (geo) satellite operator (the Geosynchronous Operational Environmental Satellites [GOES], United States; the Geosynchronous Meteorological Satellite [GMS] and then the Multi-functional Transport Satellite [MTSat] and Himawari, Japan; and the Meteorological Satellite [Meteosat], European Community). The NOAA/NCDC undertook the task of providing convenient access to these data by remapping the data to a equal-angle latitude/longitude grid, recalibrating the data to optimize homogeneity over time, correcting for biases due to varying zenith view angles, and reformatting the data for broad public distribution. As a bonus, they incorporated additional geosynchronous data that extend the record back to 1980 (although not globally complete). The resulting Gridded Satellite (GridSat) dataset provides observations recorded by three different sensor channels. Two of these channels (visible and IR) have been used on the geosynchronous satellites from the beginning of the record, and the third (water vapor) came into general use in the 1990s. The TMPA only uses the IR.

These data are used as input to TMPA processing for the period before the start of Merged 4-Km IR Tb data, currently reprocessed to start 17 February 2000. Before use, the GridSat-B1 IR Tb's are averaged to a single Tb value for the 0.25° grid box. The Indian Ocean sector lacks a satellite before 16 June 1998, when the Meteosat-5 was repositioned to that region. High-zenith-angle observations from adjacent satellites are used for fill-in as available. As well, a few residual issues remain with zenith calibration at high angles.

.....

The \*Merged 4-Km IR Tb data set\* is produced by the Climate Prediction Center (CPC), NOAA National Centers for Environmental Prediction, Washington, DC under the direction of P. Xie. Each cooperating geostationary (geo) satellite operator (the Geosynchronous Operational Environmental Satellites [GOES], United States; the Geosynchronous Meteorological Satellite [GMS], followed by the Multi-functional Transport Satellite [MTSat] and Himawari, Japan; and the Meteorological Satellite [Meteosat], European Community) forwards infrared (IR) imagery to CPC. Then global geo-IR are zenith-angle corrected (Joyce et al. 2001), re-navigated for parallax, and merged on a global grid. In the event of duplicate data in a grid box, the value with the smaller zenith angle is taken. The data are provided on a 4-km-equivalent latitude/longitude grid over the latitude band 60°N-S, with a total grid size of 9896x3298.

The data set was first produced in late 1999, but the current uniformly processed record is available starting 17 February 2000. CPC is working to extend the record back to January 1998.

All 5 geo-IR satellites are used, with essentially continuous coverage. GMS-5 was replaced by GOES-9 starting 01 UTC 22 May 2003, which introduced slightly different instrument characteristics. Then starting 19 UTC 17 November 2005 MTSat-1R took over, followed by MTSat-2 on 1 July 2010 and Himawari 8 at 02 UTC on 7 July 2015. Data from adjacent geo-IR satellites partially fills this shortfall.

Each UTC hour file contains 2 data fields. All geo-IR images with start times within 15 minutes of the UTC hour are accumulated in the "on-hour" field. Images with start times within 15 minutes of the UTC hour plus 30 minutes are accumulated in the "half-hour" field. The nominal

image start times for the various satellites and their assignment to half-hour fields are shown in Table 1.

Table 1. Nominal sub-satellite longitude (in degrees longitude) and image start time (in minutes past the hour) for the various geosynchronous satellites. The start times are displayed according to their assignment to either the on-hour or half-hour fields in the CPC Merged 4-Km IR Tb data set. Full-disc views are guaranteed only at 00, 03, ..., 21 UTC. These appear in the on-hour field except the Japanese satellite appears in the previous half-hour for all hours. For images not at these times, a satellite's "image" may be assembled from various operator-specified regional sectors. The Japanese satellite provides N. Hemisphere sectors (only) on-hour, except S. Hemisphere sectors (only) at 00, 06, 12, 18 UTC.

Satellite	Sub-sat. Lon.	on-hour	half-hour
GMS, MTSat, Himawari	140°E	00	30
series			
GOES-E (8, 12, 13, now 16)	75°W	45	15
GOES-W (10, 11, now 15)	135°W	00	30
Meteosat-11 (formerly 5, 7, 8,	0°E	00	30
9, 10)			
Meteosat-8 (formerly 5, 7)	41.5°E	00	30
	(63°E for 5, 7)		

These data are used as input to TMPA processing.

The Goddard Profiling Algorithm (\*GPROF\*) is based on Kummerow et al. (1996), Olson et al. (1999), and Kummerow et al. (2001). GPROF is a multi-channel physical approach for retrieving rainfall and vertical structure information from satellite-based passive microwave observations (here, TMI, AMSR-E, SSMI, and SSMIS). The GPROF-AMSR and GPROF-SSMI estimates are computed from the respective Tb's at MSFC and CSU, respectively, while the GPROF-TMI estimates are computed by PPS as 2A12. GPROF applies a Bayesian inversion method to the observed microwave brightness temperatures using an extensive library of profiles relating hydrometeor profiles, microwave brightness temperatures, and surface precipitation rates. The GPROF 2004 library depends on cloud model computations, while the GPROF2010 library is based on PR data. GPROF includes a procedure that accounts for inhomogeneities of the rainfall within the satellite field of view. Over land and coastal surface areas the algorithm reduces to a scattering-type procedure using only the higher-frequency channels. This loss of information arises from the physics of the emission signal in the lower frequencies when the underlying surface is other than all water.

Various versions of this algorithm are applied to the TMI, AMSR-E, SSMI, and SSMIS Tb data, and the estimates are used as input to TMPA processing. At the time Version 7 began, the most current GPROF was GPROF2010. The TMI estimates are computed using GPROF-TMI Version 7 (GPROF2010). All AMSR-E estimates have been computed using Version 10/11 of GPROF-AMSR (GPROF2004). The SSMI estimates are computed using GPROF2010-SSMI.

12

The SSMIS estimates are computed with a modification of GPROF2004 by D. Vila (which we have named GPROF2004v; Vila et al. 2013) that accounts for navigation and scan-strategy differences, calibrates the Ta's for all channels to approximate the behavior of coincident SSMI Ta's, and develops 85-GHz proxy channels from the SSMIS 91 GHz channels. The calibration to SSMI first applies "scan correction coefficients" to each of the SSMIS channels, which adjust the Ta value by a scale factor that is very close to 1.0, but which varies by field of view. This has to do with achieving scan uniformity, because the Ta values tend to drop off at the edge of the scan. Second, a histogram match is applied to the Ta's, dependent on surface type, to make the SSMIS values look like SSMI. This is done separately for the 19, 22, 37, and 91 GHz Ta's. Finally, there is a Ta-to-Tb conversion (presumably the one used in NESDIS to do the conversion for SSMI).

.....

The Version 7 PPS algorithm \*2A12\* contains Level 2 (scan-pixel) GPROF2010 estimates of precipitation based on TMI data. These are provided by PPS. Each file contains an orbit of estimates. The data have had some quality control, and are converted from sensor units to Ta, then to Tb, then to precipitation.

These data are used as input to TMPA processing.

\*SSMI Level 2 precipitation estimates\* are those produced by Colorado State University.

These estimates are computed on Level 1c SSMI brightness temperatures using GPROF 2010. Level 1c is defined as Level 1b with (potentially) different calibrations applied than the original source.

.....

\*SSMIS Level 1b Ta data\* are those archived by NOAA National Climatic Data Center, which are the operational NOAA data, essentially as produced by Fleet Numerical Meteorological and Oceanographic Center, Monterey, CA.

These data are used as input to GPROF2004v-SSMIS, which was developed as modifications to GPROF2004 by D. Vila (which we therefore named GPROF2004v; Vila et al. 2013) and further modified to run at PPS (see "GPROF").

.....

PPS algorithm \*2B31\* contains Level 2 (scan-pixel) output from the Version 7 combined PR-TMI retrieval algorithm, computed at PPS. The TRMM Combined Algorithm (TCI) combines data from the TMI and PR to produce the best rain estimate for TRMM. Currently, it uses the low frequency channels of TMI to find the total path attenuation. This information is used to constrain the radar equation. Each file contains an orbit of TCI rain rate and path-integrated attenuation at 4 km horizontal and 250 m vertical resolutions over a 220 km swath. More information is available at

http://disc.gsfc.nasa.gov/precipitation/TRMM\_README/TRMM\_2B31\_readme.shtml

and Haddad et al. (1997a,b).

These Level 2 data are used as input to TMPA processing. Production ended in early October 2014 when fuel exhaustion allowed TRMM to descend below the orbital altitude where the fixed range bins for the PR usefully saw near-surface data.

.....

The \*AMSU-B precipitation data set\* is computed operationally at the National Environmental Satellite Data and Information Service (NESDIS) Microwave Surface and Precipitation Products System (MSPPS) based on the Zhao and Weng (2002) and Weng et al. (2003) algorithm. Ice water path (IWP) and particle effective diameter size (De) are computed from the 89 and 150 GHz channels. As such, it is a primarily a scattering approach. Surface screening is carried out using Advanced Very High Resolution Radiometer (AVHRR) infrared data and Global Data Assimilation System (GDAS) surface temperature and surface type data to discriminate desert, snowy, or icy surfaces. Precipitation rate is computed based on IWP—precipitation rate relations derived from the NCAR/PSU Mesoscale Model Version 5 (MM5). The precipitation rate is approximated as a second-degree polynomial in IWP, with coefficients that are derived separately for convective and non-convective situations, based upon a series of comparisons between the three AMSU-B channels centered at the 183.31 GHz water vapor absorption band. Additionally, the algorithm identifies regions of falling snow over land through the use of AMSU-A measurements at 53.8 GHz. At present, falling snow is assigned a rate of 0.1 mm/hr, although an experimental snowfall rate is being tested and evaluated.

The data set was first produced in early 2000, last upgraded on 31 May 2007, and subsequently reprocessed. In the latter, an emission component was added to increase the areal coverage of precipitation over oceans through the use of a liquid water estimation using AMSU-A 23.8 and 31 GHz (Vila et al. 2007). Additionally, an improved coastline precipitation rate module was added that computes a proxy IWP using the 183 GHz bands (Kongoli et al. 2007). Version 6 TMPA was unable to take advantage of the uniform reprocessing, but it is used in Version 7. As a result, oceanic precipitation estimates in Version 7 are improved over Version 6 for the period 2001-2007.

These Level 2 data are used as	s input to TMPA processing	ng.
--------------------------------	----------------------------	-----

The \*MHS precipitation data set\* is computed operationally at the National Environmental Satellite Data and Information Service (NESDIS) Microwave Surface and Precipitation Products System (MSPPS) based on the algorithm previously developed to compute the AMSU-B precipitation data set (which see for details). The channel differences between the sensors are accounted for by computing synthetic 150 and 183±7 GHz channels before the precipitation is computed.

Т	he	se	Lev	vel 2	2 (	data	are	use	d as	inpu	t to	TMPA	proce	ssing.

The \*random error\* is computed for both the 3-hr (3B42) and monthly (3B43) datasets, although it is misleadingly labeled "relativeError" for historical reasons. The units are mm/hr.

The monthly random error is computed as in Huffman (1997), with appropriate adjustments for the difference in gridbox size. The 3-hr random error is similarly computed, even though the approach is not entirely consistent for such fine scales. [The Huffman (1997) approach assumes that the various input data are statistically independent.] As a partial compensation, the 3-hr random errors are approximately scaled to aggregate to the monthly random error, assuming that the 3-hr values are statistically independent. This is also not strictly true, but the overall result appeared useful.

Work is currently underway with NASA funding to develop more-appropriate estimators for random error, and to introduce estimates of bias error.

.....

The variable \*relativeError\* is so-named for historical reasons, but is actually a misnomer. The contents of the variable are actually the "random error" (in mm/hr), which the reader should consult for a summary.

.....

The High Quality (\**HQ*\*) combined microwave precipitation estimate provides a global 0.25°x0.25° -averaged 3-hourly combination of all currently available TCI, TMI, SSMI, SSMIS, AMSR-E, AMSU-B, and MHS estimates:

- 1. The GPROF-SSMI, GPROF-SSMIS, GPROF-AMSR, AMSU-B, MHS, 2A12, 2A25, and 2B31 estimates are gridded to a 0.25°x0.25° grid for a 3-hour period centered on the major synoptic times (00, 03, ..., 21 UTC). The 2A12 data are thresholded at 0.1 mm/hr to control excessive occurrence of precipitation. All of the following steps are carried out with these gridded fields.
- 2. Offline, the GPROF-SSMI, GPROF-SSMIS, GPROF-AMSR, AMSU-B, and MHS precipitation estimates have been climatologically probability-matched to 2A12. The calibrations of AMSU-B, MHS, SSMI, and AMSR-E to TMI have one set of coefficients for each sensor type for land and 14 sets for ocean, while SSMIS is calibrated separately for each satellite, again having one set for land and 14 for ocean. The ocean latitude bands are 15° overlapping latitude bands centered on the 5° bands 35-30°S, 30-25°S, 25-20°S, ..., 20-25°N, 25-30°N, and 30-35°N. The outermost bands are used in their respective hemispheres for all higher-latitude calibrations due to the lack of TMI data beyond about 38°. The SSMIS are calibrated individually due to particular calibration issues for each satellite. AMSR-E uses a 2-month set of match-ups to ensure sufficient sampling, while all of the others work with single-month accumulations. The coefficients are computed separately for each season. Finally, a volume adjustment factor is computed for each set to ensure that total TMI precipitation is preserved in these transformations.
- 3. The GPROF-SSMI, GPROF-SSMIS, GPROF-AMSR, AMSU-B, and MHS estimates are climatologically calibrated to 2A12.
- 4. The 2A12 is calibrated to the 2B31 using a matched histogram correction computed afresh for each month. The correction is computed and applied on 1° blocks since the 2A12 and

15

- 2B31 estimates vary significantly by region and time of year. The end of routine PR data on 8 October 2014 terminated the TCI as well, preventing such routine calibration after September 2014. [PR data were briefly available from 12 February to 1 April 2015 as TRMM descended past its original altitude of 350 km, but were not used in TMPA.] The 3B42/43 system was continued by shifting to a climatological calibration, as described in "TRMM end of mission issues".
- 5. The (climatologically) 2A12-calibrated GPROF-SSMI, GPROF-SSMIS, GPROF-AMSR, AMSU-B, and MHS estimates are calibrated to 2B31 using the same method as in the 2B31/2A12 adjustment scheme, but month-by-month.
- 6. The precipitation rate in each grid box is the average of 2B31, if available in the 3-hour window, or the pixel-weighted average of the calibrated conical-scan microwave radiometer estimates (2A12, GPROF-SSMI, GPROF-SSMIS, and GPROF-AMSR) contributing during the 3 hours, or the pixel-weighted average of AMSU-B and MHS estimates if no other HQ estimates are available. Most of the time there's only one overpass some time during the dataset's 3-hour window of whatever the "best" type of sensor is, and so the value is generally one snapshot spatially averaged over the grid box. As an aside, the histogram of rain rates is sensitive to averaging one, two, or three overpasses in a 3-hour period, so in IMERG we will be using only the "best" sensor closest to the mid-point of the IMERG time window (30 minutes). As noted below in HQ+VAR, if no HQ is available, the final combined estimate is given the single IR snapshot estimate at the nominal (i.e., center) time of the dataset.
- 7. Additional fields in the intermediate data file include the number of pixels, the number of pixels with non-zero rain, the number of pixels for which the estimate is "ambiguous," or highly uncertain, the instrument type producing the estimate, and the time of the instrument's overpass.
- 8. All of the HQ algorithms are unable to provide estimates in regions with frozen or icy surfaces.

The Variable Rainrate (\**VAR*\*) IR precipitation estimate converts 0.25°x0.25°-averaged geo-IR Tb to rainrates that are HQ-calibrated locally in time and space:

- 1. Both geo-IR Tb and HQ are averaged to 0.25°x0.25° to ensure consistent spatial scale, and time-space matched data are accumulated over calendar months.
- 2. In each calibration, the Tb-rainrate curve is set locally by probability matching the month's histograms of coincident IR Tb and HQ rain rate.

The local VAR Tb-rainrate curve is applied to each geo-IR Tb data set in the month:

- 1. For the Merged 4-Km Tb, over most of the globe the on-hour data field is taken as the input data, with fill-in by the previous half-hour image. The exception is the GMS sector, where the previous half-hour is primary, since GMS does not schedule images on the hour. [In that case, much of the GMS sector is filled with data from METEOSAT5 and GOES-W at very high zenith angles.] For the GridSat-B1 IR Tb there is no choice needed.
- 2. The Tb-to-rainrate conversion is a simple look-up, using whatever set of VAR calibration coefficients is current.

For the period 1 January 1998 – 16 February 2000, 10-km (subsampled), 3-hourly grids of IR data were used in the 3B42 processing. For the period 1 January 1998 - 03 UTC 16 June 1998 geo-IR data were not available in the Indian Ocean sector, but high zenith angle data from adjacent geo-satellites is generally sufficient for fill-in.

.....

The combination of \*HQ+VAR\* is computed every 3 hours from that hour's HQ and VAR fields:

- 1. The present combination scheme is to take the HQ field wherever it is non-missing, and fill in with the single-snapshot VAR at the nominal datafile time elsewhere.
- 2. The additional fields in the file are the random error of the estimate (see "random error" for a summary), the instrument type that produced the estimate, and the time of the instrument's overpass.
- 3. The VAR estimates are only posted for the latitude band 50°N-S.

These data are output as product 3B42 in TMPA processing

- 4. It is planned to do a more sophisticated combination in a future release.
- 5. Following the computation of the monthly SG combination (3B42, see "SG combination" for details), in each grid box all of the available 3-hourly HQ+VAR values are scaled to (approximately) sum to the monthly SG value.

in the control of the
*3B42* is the official PPS identifier of the 3-hour merged microwave satellite estimates (HQ) and infrared satellite estimates (VAR) data set (HQ+VAR) which are rescaled to the monthly surface precipitation gauge data. The identifier indicates that it is a level 3 (gridded) product with input from multiple sensors ("B") using non-TRMM data ("40"- series).

The monthly satellite-gauge, or \*SG combination\* is computed as follows:

- 1. The original (i.e., before the scaling step) 3-hourly HQ+VAR estimates are summed for the calendar month.
- 2. The monthly precipitation gauge analysis is used to create a large-scale (29x29 0.25° grid boxes) bias adjustment to these satellite-only estimates in regions where the gauge stations are available, mostly land. Note that analysis values distant from any gauges are not used.
- 3. The monthly gauge-adjusted satellite-only estimate is combined directly with the precipitation gauge analysis using inverse error variance weighting.

The random error is also computed as a separate field following Huffman (1997). See "random error" for a summary.

These	data ar	e output	as 3B43	in TMPA	processing.

\*3B43\* is the official PPS identifier of the monthly satellite-gauge (SG) combination data set. The identifier indicates that it is a level 3 (gridded) product with input from multiple sensors ("B") using non-TRMM data ("40"-series)

.....

The \*units of the TMPA estimates\* are mm/hour for the precipitation and random error estimates, and minutes from the nominal observation time for the observation time field. The precipitation values are based on satellite snapshots. These might be thought of as an instantaneous rate, valid at the nominal observation time, although Villarini and Krajewski (2007) showed that 3B42 is best correlated with radar data averaged over 60-90 minutes, not always centered on the nominal overpass time. The SG combination (3B43) precipitation value is an average rate over the month.

.....

The \*3B42 data fields\* provide a variety of information for users and data developers:

Table 2. List of data fields, their variable names (in the data structure), and the data units for 3B42 data files.

f = f = f = f = f = f = f = f = f = f =							
Index	Data field	Variable name	Units				
1	precipitation	precipitation	mm/hr				
2	precipitation random error*	relativeError	mm/hr				
3	satellite observation time	satObservationTime	min. from nominal				
4	HQ precipitation	HQprecipitation	mm/hr				
5	IR precipitation	IRprecipitation	mm/hr				
6	satellite precipitation source	satPrecipitationSource	n/a				

<sup>\*</sup> Note the mismatch between the data field "random error" and the assigned variable name "relativeError". The first is accurate.

The coding in the source field matches that in the 3B42RT file, which is as follows:

0 = no observation	1 = AMSU	2 = TMI
3 = AMSR	4 = SSMI	5 = F17 SSMIS
6 = MHS	7 = TCI	8 = MetOp-B
9 = spare sounder  2	10 = spare sounder  3	11 = F16 SSMIS
12 = F18 SSMIS	13 = spare scanner  6	30 = AMSU&MHS avg.
31 = conical avg.	50 = IR	1,2,,12 + 100 = sparse-sample HQ

Because the data are provided at nominal UTC hours, each 3B42 data set represents a nominal +/-90-minute span around the nominal hour. Thus, the 00 UTC images include data from the very end of the previous UTC day.

For historical reasons, this coding is slightly different than that for the TMPA-RT.

The \*3B43 data fields\* provide a variety of information for users and data developers:

Table 3. List of data fields, their variable names (in the data structure), and the data units for 3B43 data files.

Index	Data field	Variable name	Units
1	precipitation	precipitation	mm/hr
2	precipitation random error*	relativeError	mm/hr
3	gauge relative weighting	gaugeRelativeWeighting	fraction

<sup>\*</sup> Note the mismatch between the data field "random error" and the assigned variable name "relativeError". The first is accurate.

Because the input HQ data are provided at nominal UTC hours, the 3B43 data set is built with a nominal +/-90-minute span around the nominal hour. Thus, a month of 3B43 month contains 90 minutes of information into the previous and next months with half weighting.

.....

The Merged Multi-satelliE Retrievals for GPM (\*IMERG\*) is being developed as a unified U.S. algorithm for the Day-1 multi-satellite precipitation product by the U.S. GPM team. The precipitation estimates computed from the various precipitation-relevant satellite passive Microwave (PMW) sensors are using GPROF2017 computed at the Precipitation Processing System (PPS) as is now done for the TRMM Multi-satellite Precipitation Analysis (TMPA). These estimates are gridded and intercalibrated, then combined into half-hourly fields and provided to both the Climate Prediction Center (CPC) Morphing-Kalman Filter (CMORPH-KF) Lagrangian time interpolation scheme and the Precipitation Estimation from Remotely Sensed Information using Artificial Neural Networks – Cloud Classification System (PERSIANN-CCS) re-calibration scheme. In parallel, CPC assembles the zenith-angle-corrected, intercalibrated "even-odd" geo-IR fields and forward them to PPS for use in the CMORPH-KF Lagrangian time interpolation scheme and the PERSIANN-CCS computation routines. The PERSIANN-CCS estimates are computed (supported by an asynchronous re-calibration cycle) and sent to the CMORPH-KF Lagrangian time interpolation scheme. The CMORPH-KF Lagrangian time interpolation (supported by an asynchronous KF weights updating cycle) uses the PMW and IR estimates to create half-hourly estimates. The system will be run twice in near-real time

- "Early" multi-satellite product ~4 hr after observation time and
- "Late" multi-satellite product ~14 hr after observation time,

and once after the monthly gauge analysis is received

• "Final" satellite-gauge product ~3 months after the observation month.

The baseline is for the (near-)real-time "Early" and "Late" estimates to be calibrated with climatological coefficients that vary by month and location, while in the "Final" post-real-time run the multi-satellite estimates are adjusted so that they sum to a monthly satellite-gauge combination following the TMPA. In all cases the output contains multiple fields that provide information on the input data, selected intermediate fields, and estimation quality. For more details see the IMERG ATBD (Huffman et al. 2017), posted at

https://pmm.nasa.gov/sites/default/files/document\_files/IMERG\_ATBD\_V5.2.pdf .

## 6. Temporal and Spatial Coverage and Resolution

19

The \*file date\* is the UTC year, month, day in which the nominal time of the 3B42 data set occurs, or the UTC year, month that 3B43 represents. All dates and times are UTC.

.....

The \*temporal resolution\* of the products is:

• HQ+VAR (3B42): 3 hr

• SG (3B43): monthly

The 3-hour period for the HQ+VAR (3B42) is driven by the need for the HQ to accumulate a reasonable sample without encompassing too large a fraction of the diurnal cycle. Note that both the microwave and IR data are snopshots, except for small regions in which two (or more) overlapping microwave scenes are averaged in the HQ field. This is done to make the statistics of the data sets as comparable as possible. The precipitation values are based on satellite snapshots. These might be thought of as an instantaneous rate, valid at the nominal observation time, although Villarini and Krajewski (2007) showed that 3B42 is best correlated with radar data averaged over 60-90 minutes, not always centered on the nominal overpass time. The SG combination (3B43) precipitation value is an average rate over the month.

The monthly period for the SG (3B43) is driven by the typical monthly period of precipitation gauge analyses, although it is also a typical period requested by many users. The precipitation value is an average over the month.

.....

The \*period of record\* for the TMPA is January 1998 through the present, with a delay of about two months after the end of the month for processing. The start is based on the first full month of TRMM data. Note that the very first 3-hour period (00 UTC on 1 January 1998) lacks data from 1997, so it only has 1.5 hours of data, 0000-0130 UTC. The real-time TRMM product 3B42RT provides real-time processing of the TMPA from early February 2000 to the present. See "3B42RT" for more details.

.....

The \*grid\* on which each field of values is presented is a 0.25°x0.25° lat./lon. (Cylindrical Equal Distance) global array of points. It is size 1440x400, with X (longitude) incrementing most rapidly West to East from the Dateline, and then Y (latitude) incrementing South to North from the southern edge. Quarter-degree latitude and longitude values are at grid edges:

First point center (49.875°S,179.875°W) Second point center (49.875°S,179.625°W) Last point center (49.875°N,179.875°E)

The reference datum is WGS84.

.....

The \*spatial resolution\* of the TMPA is 0.25°x0.25° lat/lon.

.....

The \*spatial coverage\* of the TMPA is 50°N-S.

20

### 7. Production and Updates

\*Production and updates\* for the TMPA are a joint activity of the precipitation research group in NASA Goddard Space Flight Center in the Mesoscale Atmospheric Processes Laboratory and PPS

The latency of the products after the month is governed by the latency of the individual input products. At this time the pacing item is the delivery of the gauge analysis. Once initiated, the processing occurs in a matter of minutes.

Updates will be released to (1) extend the data record, (2) take advantage of improved combination techniques, or (3) correct errors. Updates resulting from the last two cases will be given new version numbers.

NOTE: The changes described in this section are typical of the changes that are required to keep the TMPA abreast of current requirements and science. Users are strongly encouraged to check back routinely for additional upgrades and to refer other users to this site rather than redistributing data that are potentially out of date.

The TRMM satellite was boosted from an altitude of 350 km to 401.5 km over the period 7-14 August 2001 to lengthen the life of the mission, in fact more than doubling it. This change slightly degraded the instrument resolution. Subsequently, the various algorithms were modified to account for as many of the effects as possible, although residuals are noticeable in some cases.

The TRMM PR suffered an electronics failure on 29 May 2009. Data were lost until the "B-side" electronics were activated 19 June 2009. Some residual differences are noticeable.

In some cases, such as the failure of AMSR-E, the end of a data record is clear. In other cases, such as the gradual failure of the NOAA-16 AMSU-B during 2010, the point at which to end use of the data is a matter of judgment. In the latter case we chose 30 April 2010 despite continued operation into early 2011. [This is a direct transfer of experience from the 3B42RT product.]

As described in "additional processing for Version 7", the initial retrospective processing accidentally omitted AMSU and MHS data. As a result, an immediate retrospective processing was carried out without a change in version number, although the version identifier contained in file names from the retrospective part of the processing is now "7A" instead of "7".

As described in "TRMM end of mission issues", the calibration to 2B31 shifted from using coincident data to a climatological calibration as of October 2014.

In the future,	all products	will be prov	vided with	random e	error estima	ates.

Several \**TRMM end of mission issues*\* impact the TMPA 3B42/43 system:

26 April 2018 TRMM 3B42\_3B43\_doc 21

- 1. On 7 October 2014, routine production ended for the TRMM PR precipitation estimates due to the ongoing descent and ultimate decommissioning of the TRMM satellite (PMM, 2014). [PR data were briefly available from 12 February to 1 April 2015 as TRMM descended past its original altitude of 350 km, but were not used in TMPA.] Estimates from the TMI continued to be produced until it was turned off on 8 April 2015 as part of the TRMM decommissioning. Since PR was no longer available, the TCI estimates are also no longer available. As the research version of the TMPA (products 3B42 and 3B43) uses the TCI estimates as the satellite calibrator, September 2014 was the last month these products were produced in this way. Note that the real-time TMPA (TMPA-RT – products 3B40RT, 3B41RT and 3B42RT) uses climatological satellite calibrations, so continues despite the loss of TRMM estimates. In an effort to keep the research version of TMPA available and usable, we adapted the TMPA-RT climatological calibrations/adjustments for use in the research products. October 2014 is the first month of the climatologically calibrated/adjusted research TMPA (Huffman and Bolvin 2015). Users should note there will be a discontinuity in the research TMPA record as a result, the degree of which will be provided by analysis of test results generated for the period October 2013 – September 2014. These months of test data can be provided to users upon request. Each individual user must determine the most appropriate use of the climatologically calibrated/adjusted 3B42 and 3B43 products, based on the comparison results provided below and the user's own analysis. We encourage users to report their findings to the developers for the benefit of the community.
- 2. TMI continued to be included as one of the input data sets until it was ended on 8 April 2015 as part of the TRMM decommissioning activities.
- 3. Despite the end of TRMM operations, the successor IMERG will not be a complete replacement until retrospective processing is carried out in early 2017. Giving a decent interval for users to make the transition argues for continuing TMPA production until mid-2017.

#### 8. Sensors

The TRMM Precipitation Radar (\*PR\*) is a flat-panel phased-array weather radar, the first flown in space. TRMM is placed in a (46-day) precessing orbit at a 35° inclination with a period of about 91.5 min. The horizontal and vertical resolutions are 4 km and 250 m, respectively, over a 220 km swath to a height above sea level of 20 km. The minimum detectable signal is 17 (18) dBZ before (after) the TRMM orbit boost in August 2001. The TRMM PR suffered an electronics failure on 29 May 2009. Data were lost until the "B-side" electronics were activated until 19 June 2009. Some residual differences are noticeable. As summarized in "TRMM end of mission issues", regular computation of PR data ended on 8 October 2014.

The PR is an operational sensor, so the data record suffers the usual gaps in the record due to processing errors, down time on receivers, etc. There were outages for an operational anomaly in May 2000, and the boost to a higher orbit during the first part of August 2001.

22

The 35° inclination provides nominal coverage over the latitudes 37°N-S.

Further details are available in Kummerow et al. (1998).

The TRMM Microwave Imager (\**TMI*\*) is a multi-channel passive microwave radiometer that flies on TRMM. TRMM is placed in a (46-day) precessing orbit at a 35° inclination with a period of about 91.5 min. The TMI provides vertical and horizontal polarization values for 10.65, 19.35 21.3, 37.0, and 85.5 GHz frequencies (except only vertical at 21) with conical scanning, similar to the SSMI. The channels have effective fields of view that vary from 4.6x6.9 km for the 85 GHz (oval due to the slanted viewing angle intersecting the surface at 51°) to 29.1x55.2 km for the 10 GHz. Consequently, the 85 GHz is undersampled near nadir, and all other channels are more or less oversampled. At the swath edge even the 85.5 GHz is oversampled.

The TMI is an operational sensor, so the data record suffers the usual gaps in the record due to processing errors, down time on receivers, etc. There were outages for an operational anomaly in May 2000 and the boost to a higher orbit during the first part of August 2001. As summarized in "TRMM end of mission issues", regular computation of TMI data ended on 8 April 2015.

The 35° inclination provides nominal coverage over the latitudes 40°N-S, although limitations in retrieval techniques prevent useful precipitation estimates in cases of cold land or sea ice (which is unlikely in this latitude range).

Further details are	available	in Kummerow	et al.	(1998).
---------------------	-----------	-------------	--------	---------

.....

The Advanced Microwave Scanning Radiometer for the Earth Observing System (\*AMSR-E\*) is a multi-channel passive microwave radiometer provided by the Japan Aerospace Exploration Agency that flew on Aqua from mid-2003 until it failed in late 2011. Data use in 3B42/43 cover 19 June 2002 – 3 October 2011. Aqua is placed in a sun-synchronous polar orbit with a period of about 102 min. The AMSR-E provided vertical and horizontal polarization values for 6, 10, 18, 23, 36, and 89 GHz frequencies (except only vertical at 23) with conical scanning, similar to the SSMI. Pixels and scans were spaced 10 km apart at the suborbital point, except the 89-GHz channels were collected at 5 km spacing. However, the B-scan sensor, which provides the 89 GHz scan between the lower-frequency scans, failed around 4 November 2004. Every other high-frequency pixel was co-located with the low-frequency pixels, starting with the first pixel in the scan and the first scan in a pair of scans. The channels had resolutions that vary from 4x6 km for the 89 GHz (oval due to the slanted viewing angle) to 43x74 km for the 6 GHz.

The polar orbit provides nominal coverage over the latitudes 85°N-S, although limitations in current retrieval techniques prevent useful precipitation estimates in cases of cold land or sea ice.

The AMSR-E was an operational sensor, so the data record suffered the usual gaps in the record due to processing errors, down time on receivers, etc. Over time the coverage improved as the operational system matured. As noted above, the B-scan sensor failed around 4 November 2004.

Further	details	are ava	ailable at	http://www	.ghcc.	msfc.na	sa.gov/Al	MSR/.

26 April 2018 TRMM 3B42\_3B43\_doc 23

The Special Sensor Microwave/Imager (\*SSMI\*) is a multi-channel passive microwave radiometer that has flown on selected Defense Meteorological Satellite Program (DMSP) platforms since mid-1987. The DMSP is placed in a sun-synchronous polar orbit with a period of about 102 min. The SSMI provides vertical and horizontal polarization values for 19, 22, 37, and 85 GHz frequencies (except only vertical at 22) with conical scanning. Pixels and scans are spaced 25 km apart at the suborbital point, except the 85-GHz channels are collected at 12.5 km spacing. Every other high-frequency pixel is co-located with the low-frequency pixels, starting with the first pixel in the scan and the first scan in a pair of scans. The channels have resolutions that vary from 12.5x15 km for the 85 GHz (oval due to the slanted viewing angle) to 60x75 km for the 19 GHz.

The polar orbit provides nominal coverage over the latitudes 85°N-S, although limitations in current retrieval techniques prevent useful precipitation estimates in cases of cold land or sea ice.

The SSMI is an operational sensor, so the data record suffers the usual gaps in the record due to processing errors, down time on receivers, etc. Over time the coverage has improved as the operational system has matured. As well, the first 85 GHz sensor to fly degraded quickly due to inadequate solar shielding. After launch in mid-1987, the 85.5 GHz vertical- and horizontal-polarization channels became unusable in 1989 and 1990, respectively. Another issue arose on 14 August 2006: DoD activated the RADCAL beacon on the F15 DMSP, which interfered with the 22V and 85.5V channels, preventing reliable estimates using current GPROF code.

Further details are available in Hollinger et al. (1987, 1990). Note that the acronym was originally "SSM/I", but "SSMI" has since come into common use.

Table 4. The inventory of SSMI data used in the TMPA, period of record, and sensor status.

DMSP	Period of Record	Status
F13	1 January 1998 - 31 July 2009	inactive
F14	1 January 1998 - 23 August 2008	inactive
F15	23 February 2000 - 14 August 2006	active, but unusable

.....

The Special Sensor Microwave Imager/Sounder (\*SSMIS\*) is a multi-channel passive microwave radiometer that has flown on selected Defense Meteorological Satellite Program (DMSP) platforms since late 2003. The DMSP is placed in a sun-synchronous polar orbit with a period of about 102 min. The SSMIS provides vertical and horizontal polarization values for the SSMI-like 19, 22, 37, and 91 GHz frequencies (except only vertical at 22) with conical scanning, as well as other channels with a heritage in the Special Sensor Microwave/Temperature 2 (SSM/T2) sensor. Unlike SSMI, every SSMIS scan observes at all channels: pixels and scans are respectively spaced 25 and 12.5 km apart at the suborbital point for channels below 91 GHz, 12.5 km for both pixel and scans for 91 GHz. Thus, the high-frequency channels have twice as many footprints per scan as the lower-frequency channels. Separate feed horns are used for 91 GHz and the rest of the SSMI-like frequencies, so there is not a 1:1 co-location of channel values, as there is for SSMI. The SSMI-like channels have the resolutions

46.5x73.6 km (19, 22 GHz) 31.2x45.0 km (37 GHz) 13.2x15.5 km (91 GHz)

with the slanted viewing angle and in-line processing determining the oval shape.

Operational and design problems early in the program raised serious obstacles to use of the data. Accordingly, the useful periods of record (below) start relatively long after launch. These dates are based on the start of the first publicly available SSMIS as determined by NRL/FNMOC through the Shared Processing Program with NESDIS. In the current version we apply the approximate calibrations developed by D. Vila as part of GPROF2004v (Vila et al. 2013). See "GPROF" for a short summary.

The polar orbit provides nominal coverage over the latitudes 85°N-S, although limitations in current retrieval techniques prevent useful precipitation estimates in cases of cold land or ice.

The SSMIS is an operational sensor, so the data record suffers the usual gaps in the record due to processing errors, down time on receivers, etc. Over time the coverage has improved as the operational system has matured.

Further details are available in Northrup Grumman (2002). Note that the acronym was originally "SSMI/S", but "SSMIS" has since come into common use.

Table 5.	The inventory of SSMIS data used in the TMPA, period of record,			
and sensor status.				

DMSP	Period of Record	Status
F16	20 November 2005 - ongoing	active
F17	19 March 2008 - ongoing	active
F18	8 March 2010 - ongoing	active

.....

The Advanced Microwave Sounding Unit B (\*AMSU-B\*) is a multi-channel passive microwave radiometer that flew on selected National Oceanic and Atmospheric Administration (NOAA) platforms from early 2000 to 2011. The NOAA satellites are placed in sun-synchronous polar orbits with periods of about 102 min. The complete AMSU contained 20 channels, the first 15 referred to as AMSU-A, and the last 5 as AMSU-B. These channels (identified as 16 through 20) covered the frequencies 89.0±0.9, 150.0±0.9, and 183.31±1, 3, and 7, all in GHz, with crosstrack scanning. Pixels and scans were spaced 16.3 km apart at nadir, with the pixels increasing in size and changing from circular to elongated in the cross-track direction as one moves away from nadir.

The polar orbit provides nominal coverage over the entire globe, although limitations in current retrieval techniques prevent useful precipitation estimates in cases of cold land or sea ice.

The AMSU-B was an operational sensor, so the data record suffered the usual gaps in the record due to processing errors, down time on receivers, etc. Over time the coverage improved as the operational system matured. As well, the NOAA-17 50-GHz channel failed in late October

2003, apparently due to solar flare activity. Finally, NOAA-16 gradually failed during 2010, and eventually it was determined that the Version 7 TMPA should stop using the data at the end of April 2010.

Further details are available in the NOAA KLM User's Guide (September 2000 revision) at <a href="http://www2.ncdc.noaa.gov/docs/klm/index.htm">http://www2.ncdc.noaa.gov/docs/klm/index.htm</a>, specifically at <a href="http://www2.ncdc.noaa.gov/docs/klm/html/c3/sec3-4.htm">http://www2.ncdc.noaa.gov/docs/klm/html/c3/sec3-4.htm</a>.

Table 6. The inventory of AMSU-B data used in the TMPA, period of record, and sensor status.

period of recent, and sensor status.					
Satellite	Period of Record	Status			
NOAA-15	1 January 2000 - 14 September 2010	inactive			
NOAA-16	4 October 2000 - 16 February 2011	inactive			
	(last used for 30 April 2010)				
NOAA-17	28 June 2002 - 17 December 2009	inactive			

.....

The Microwave Humidity Sounder (\*MHS\*) is a multi-channel passive microwave radiometer that has flown on selected National Oceanic and Atmospheric Administration (NOAA) platforms since mid-2005 as a follow-on to AMSU-B and on the EUMETSAT MetOp-A since late 2006. The satellites are placed in sun-synchronous polar orbits with periods of about 102 min. The MHS contains 5 channels, similar to AMSU-B. These channels cover the frequencies 89.0, 157.0, 183.311±1 and 3, and 190.311, all in GHz, with cross-track scanning. Pixels and scans are spaced 16.3 km apart at nadir, with the pixels increasing in size and changing from circular to elongated in the cross-track direction as one moves away from nadir.

The polar orbit provides nominal coverage over the entire globe, although limitations in retrieval techniques prevent useful precipitation estimates in cases of cold land or sea ice.

The MHS is an operational sensor, so the data record suffers the usual gaps in the record due to processing errors, down time on receivers, etc. Over time the coverage has improved as the operational system has matured.

Further details are available in the NOAA KLM User's Guide (September 2000 revision) at http://www2.ncdc.noaa.gov/docs/klm/index.htm, specifically at http://www2.ncdc.noaa.gov/docs/klm/html/c3/sec3-9.htm.

Table 7. Inventory of MHS data used in the TMPA, period of record, and sensor status.

	-	
Satellite	Period of Record	Status
NOAA-18	25 May 2005 – current	active
NOAA-19	25 February 2009 – current	active
MetOp-A	5 December 2006 – current	active
MetOp-B	1 July 2013 – current	active

.....

The infrared (\*IR\*) data are collected from a variety of sensors flying on the international constellation of geosynchronous-orbit meteorological satellites – the Geosynchronous

Operational Environmental Satellites (GOES, United States); the Geosynchronous Meteorological Satellite (GMS, Japan), subsequently Multi-functional Transport Satellite, (MTSat, Japan) and then Himawari (Japan); and the Meteorological Satellite (Meteosat, European Community). There are usually two GOES platforms active covering the eastern and western regions of the Americas, and two Meteoats covering the Europe/Africa and Indian Ocean sectors. The geosynchronous IR data are collected by scanning (parts of) the earth's disk. By international agreement, all satellite operators collect full-disk images at the synoptic observing times (00, 03, ..., 21 UTC) at a minimum.

Subsequent processing is described in "GridSat-B1 IR Tb data set" and "Merged 4-Km IR Tb data set".

The various IR instruments are operational sensors, so the data record suffers the usual gaps in the record due to processing errors, down time on receivers, sensor failures, etc. Most notably during the TMPA period of record, there was no geo-IR coverage in the Indian Ocean sector until 06 UTC 16 June 1998, although high-zenith-angle observations from adjacent geo-satellites are used to cover the gap. As well, GMS-5 was replaced by GOES-9 starting 01 UTC 22 May 2003, which introduced slightly different instrument characteristics. Starting 19 UTC 17 November 2005 MTSat-1R went operational, followed by a shift to MTSat-2 on 1 July 2010, and then Himawari 8 at 02 UTC on 7 July 2015.

Further details are available in Janowiak and Arkin (1991).

.....

The \*precipitation gauge analysis\* that is used in the TMPA is produced by the Global Precipitation Climatology Centre (GPCC) under the direction of Andreas Becker and Udo Schneider, located in the Deutscher Wetterdienst, Offenbach a.M., Germany (Schneider et al. 2008). [Note: Throughout, we are clearly dealing with all forms of precipitation, but we follow the customary practice here of referring to precipitation gauges as "rain gauges".] Rain gauge reports are archived from a time-varying collection of over 70,000 stations around the globe, both from Global Telecommunications System (GTS) reports and from other world-wide or national data collections. An extensive quality-control system is run, featuring an automated screening and then a manual step designed to retain legitimate extreme events that characterize precipitation. This long-term data collection and preparation activity feeds into an analysis that is done in two steps. First, a long-term climatology is assembled from all available gauge data, focusing on the period 1951-2000. The lack of complete consistency in period of record for individual stations has been shown to be less important than the gain in detail, particularly in complex terrain. Then for each month, the individual gauge reports are converted to deviations from climatology, and are analyzed into gridded values using a variant of the SPHEREMAP spatial interpolation routine (Willmott et al. 1985). Finally, the month's analysis is produced by superimposing the anomaly analysis on the month's climatology.

The GPCC creates multiple products, and two are used in the TMPA. The Full Data Reanalysis (currently Version 6) is a retrospective analysis that covers the period 1901-2010, and it is used in the TMPA for the span 1998-2010. Thereafter we use the GPCC Monitoring Product (currently Version 4), which has a similar quality control and the same analysis scheme as the

Full Data Reanalysis, but whose data source is limited to GTS reports. Compared to the Version 6 TMPA, the advantages of using GPCC data throughout are that 1) we no longer need to use the separate and differently prepared gauge analysis based on the Climate Analysis and Monitoring System (CAMS) for Initial Processing, and 2) the numbers of gauges used are much higher for most of the period of record. When the Full Data Reanalysis is updated to a longer record we hope to reprocess the TMPA datasets to take advantage of the improved data. We continue our long-standing practice of correcting all gauge analysis values for climatological estimates of systematic error due to wind effects, side-wetting, evaporation, etc., following Legates [1987]. We hope to develop a more modern and detailed correction for these effects in subsequent versions

.....

The inventory of \*sensors contributing to TMPA\* is summarized here for convenience; refer to the individual sensor descriptions for additional details.

Table 8. Inventory of sensors contributing to the TMPA data, including start/stop dates, institutional source of the sensor data and precipitation estimate, and explanatory comments. Note that the datasets starting at the beginning of 1998 do not contribute data from the end of

1997 for the first 3-hour period of 00 UTC on 1 January 1998.

Sensor	Start Date	End Date	Source	Comment(s)
AMSR-E	19 June 2002	3 Oct 2011	NSIDC AE_Rain.2 V10 GPROF	frozen at V10/V11 (GPROF2004)
SSMI DMSP F13	1 Jan 1998	31 July 2009	CSU GPROF2010 V1a	coverage too sparse later
SSMI DMSP F14	1 Jan 1998	23 Aug 2008	CSU GPROF2010 V1a	
SSMI DMSP F15	23 Feb 2000	13 Aug 2006	CSU GPROF2010 V1a	RADCAL beacon interference later
SSMIS DMSP F16	20 Nov 2005	ongoing	CLASS TDR, GPROF2004V	start of CLASS TDR archive
SSMIS DMSP F17	19 Mar 2008	ongoing	CLASS TDR, GPROF2004V	start of CLASS TDR archive
SSMIS DMSP F18	8 Mar 2010	ongoing	CLASS TDR, GPROF2004V	start of CLASS TDR archive
AMSU-B NOAA-15	1 Jan 2000	14 Sep 2010	CICS; CLASS	CICS archive before 1 June 2007
AMSU-B NOAA-16	4 Oct 2000	30 Apr 2010	CICS; CLASS	CICS archive before 1 June 2007
AMSU-B NOAA-17	28 Jun 2002	17 Dec 2009	CICS; CLASS	CICS archive before 1 June 2007
MHS NOAA-18	25 May 2005	ongoing	CICS; CLASS	CICS archive before 1 June 2007
MHS NOAA-19	25 Feb 2009	ongoing	CICS; CLASS	CLASS archive starts 7 May 2009
MHS MetOp-A	5 Dec 2006	ongoing	CICS; CLASS	CICS archive before 1 June 2007; data gap

				14 UTC 27 March 2014–0746 UTC 21
				May 2014
MHS	1 Jul 2013	ongoing	CLASS	Archive starts in May
MetOp-B	1 341 2013	ongoing	CLASS	2013
TMI	1 Jan 1998	8 Apr 2015	CSU GPROF2010 V1	
TCI	1 Jan 1998	8 Oct 2014	PPS	
IR	1 Jan 1998	1 Jan 1000 angaing D1, CDC 4lm Th		B1 before
IK	1 Jan 1998	ongoing	B1; CPC 4km Tb	17 Feb 2000
Gauga	Jan 1998	ongoing	GPCC 1°	use Full through
Gauge	Jan 1998 Ong	ongoing	Full/Monitoring	Dec 2010

### 9. Error Detection and Correction

\*PR error detection/correction\* has several parts. The performance of the various radar components, including transmit power and Low Noise Amplifiers, are monitored. An active ground calibration target is episodically viewed, and surface Zo is routinely monitored. See <a href="http://pps.gsfc.nasa.gov/tsdis/Documents/PR\_Manual\_JAXA\_V6.pdf">http://pps.gsfc.nasa.gov/tsdis/Documents/PR\_Manual\_JAXA\_V6.pdf</a> for more information.

Accuracies in the radar data are within the uncertainties of the precipitation estimation techniques.

The satellite altitude change in August 2001 introduced some changes in detectability for which the algorithms are supposed to approximately account. The TRMM PR electronics failure on 29 May 2009 resulted in a switch to the "B-side" electronics. Some residual differences are noticeable

.....

\*TMI error detection/correction\* is quite similar to that of the SSMI (below) because it is a modified SSMI with the 10 GHz channels added. Built-in hot- and cold-load calibration checks are used to convert counts to antenna temperature (Ta). An algorithm converts Ta to brightness temperature (Tb) for the various channels (eliminating cross-channel leakage). As well, systematic navigation corrections are performed. All pixels with non-physical Tb and local calibration errors are deleted.

Accuracies in the Tb's are within the uncertainties of the precipitation estimation techniques. For the most part, tests show stable cross-calibration with the fleet of SSMI's and SSMIS's.

TRMM is designed to precess over a 46-day period. There is no direct effect on the accuracy of the TMI data, but the continually changing diurnal sampling causes significant systematic fluctuations in the resulting TMI-only precipitation estimates.

One important test for artifacts is screening the data for "excessive" numbers of "ambiguous pixels"; see that topic for an explanation.

.....

\*AMSR-E error detection/correction\* has several parts. Built-in hot- and cold-load calibration checks are used to convert counts to antenna temperature (Ta). An algorithm has been developed to convert Ta to brightness temperature (Tb) for the various channels (eliminating cross-channel leakage). As well, systematic navigation corrections are performed. All pixels with non-physical Tb and local calibration errors are deleted.

Accuracies in the Tb's are within the uncertainties of the precipitation estimation techniques.

One important test for artifacts is screening the data for "excessive" numbers of "ambiguous pixels"; see that topic for an explanation.

.....

\*SSMI error detection/correction\* has several parts. Built-in hot- and cold-load calibration checks are used to convert counts to antenna temperature (Ta). An algorithm has been developed to convert Ta to brightness temperature (Tb) for the various channels (eliminating cross-channel leakage). Differences between the Ta-to-Tb conversions employed by RSS and the U.S. Navy's Fleet Numerical Meteorological and Oceanographic Center imply that uncertainties in the Ta-to-Tb conversion are much larger than any other known uncertainty. Consequently, Colorado State University developed the concept of a Level 1c, which applies corrections developed in the project. In this case, the SSMI Tb's are adjusted to perform as much like the TMI Tb's as possible. As well, systematic navigation corrections are performed. All pixels with non-physical Tb and local calibration errors are deleted.

Accuracies in the Tb's are within the uncertainties of the precipitation estimation techniques. For the most part, tests show only small differences among the SSMI sensors flying on different platforms.

Some satellites experienced significant drifting of the equator-crossing time during their period of service (see <a href="http://precip.gsfc.nasa.gov/times\_allsat.jpg">http://precip.gsfc.nasa.gov/times\_allsat.jpg</a> for a current time-series plot). There is no direct effect on the accuracy of the SSMI data, but it is possible that the systematic change in sampling time could introduce biases in any resulting SSMI-only precipitation estimates.

One important test for artifacts is screening the data for "excessive" numbers of "ambiguous pixels"; see that topic for an explanation.

.....

\*SSMIS error detection/correction\* has several parts, similar to SSMI. However, Colorado State University is not yet in a position to establish Level 1c datasets, so Ta data sets from NOAA/NCDC are employed in a correction scheme developed by D. Vila (Vila et al. 2013). Errors in the SSMIS Tb's are believed to be "small", except the F16 is known to have some unsolved issues.

In addition, F16 has experienced significant drifting of the equator-crossing time during its period of service (see <a href="http://precip.gsfc.nasa.gov/times\_allsat.jpg">http://precip.gsfc.nasa.gov/times\_allsat.jpg</a> for a current time-series plot). There is no direct effect on the accuracy of the SSMIS data, but it is possible that the systematic

30

change in sampling time could introduce biases in any resulting SSMIS-only precipitation estimates.

One important test for artifacts is screening the data for "excessive" numbers of "ambiguous pixels"; see that topic for an explanation.

.....

\*AMSU-B error detection/correction\* has several parts. Built-in hot- and cold-load calibration checks are used to convert counts to antenna temperature (Ta). Systematic navigation corrections are performed. All pixels with non-physical Tb and local calibration errors are deleted.

Accuracies in the Tb's are within the uncertainties of the precipitation estimation techniques. The main difficulty results from the loss of the NOAA-17 50-GHz channel.

Some satellites experienced significant drifting of the equator-crossing time during their period of service (see <a href="http://precip.gsfc.nasa.gov/times\_allsat.jpg">http://precip.gsfc.nasa.gov/times\_allsat.jpg</a> for a current time-series plot). There is no direct effect on the accuracy of the AMSU-B data, but it is possible that the systematic change in sampling time could introduce biases in any resulting AMSU-B-only precipitation estimates.

.....

\*MHS error detection/correction\* has several parts. Built-in hot- and cold-load calibration checks are used to convert counts to antenna temperature (Ta). Systematic navigation corrections are performed. All pixels with non-physical Tb and local calibration errors are deleted.

Accuracies in the Tb's are within the uncertainties of the precipitation estimation techniques.

Some of the relevant satellites are beginning to drift in the equator-crossing time during their periods of service (see <a href="http://precip.gsfc.nasa.gov/times\_allsat.jpg">http://precip.gsfc.nasa.gov/times\_allsat.jpg</a> for a current time-series plot). There is no direct effect on the accuracy of the MHS data, but it is possible that the systematic change in sampling time could introduce biases in any resulting MHS-only precipitation estimates.

.....

In common with some other microwave algorithms, GPROF flags pixels with certain ranges of Tb values as \*ambiguous pixels\* because such ranges are associated with both real precipitation and artifacts, compared to coincident weather observations. In this approach, the algorithm makes an estimate, but flags it as a possible artifact. GPROF leaves it to the user to evaluate such pixels for use or deletion. Experience shows that if an artifact due to surface effects is responsible, it tends to trigger ambiguous values in the same place repeatedly, and one can capture this by seeing how many of the pixels in the area are flagged. The threshold of "too many" ambiguous pixels is somewhat subjectively chosen to balance dropping good data and including artifacts. In the TMPA the ambiguous pixels are handled as follows:

31

- 1. In the HQ, experience shows that when the fraction of ambiguous (FA) exceeds 40% or the 5x5-grid box average FA exceeds 5%, the precipitation value is likely an artifact.
- 2. In the calibration for VAR, all flagged precipitation values are accumulated along with the presumably good values. Experience shows that the month-accumulated values should be discarded when accumulated FA exceeds 20%, or the 5x5-grid-box-average accumulated FA exceeds 10%, or the grid box has fewer than 60% of the nominal number of samples for the month at the box's latitude. The resulting holes in the coefficient field are smooth-filled from surrounding grid boxes. In some cases, such as January in Eurasia, these fill-ins can be quite extensive. As a result, our confidence in VAR over wintertime land is reduced.
- 3. In the combination of HQ and VAR, the HQ values previously judged to be suspect are set to missing before combination with VAR.

The dominant \*IR data correction\* is for slanted paths through the atmosphere. Referred to as "limb darkening correction" in polar-orbit data, or "zenith-angle correction" (Joyce et al. 2001) in geosynchronous-orbit data, this correction accounts for the fact that a slanted path through the atmosphere increases the chances that (cold) cloud sides will be viewed, rather than (warm) surface, and raises the altitude dominating the atmospheric emission signal (almost always lowering the equivalent Tb). The slant path also creates an offset to the geolocation of the IR pixel due to parallax. That is, the elevated cloud top, viewed from an angle, is located closer to the satellite than where the line of sight intersects the Earth's surface. Pixels are moved according to a standard height-Tb-zenith angle profile, at the price of holes created when tall clouds are moved farther than shallow clouds behind them. In addition, the various sensors have a variety of sensitivities to the IR spectrum, usually including the 10-11 micron band. Intersatellite calibration differences are documented, but they are not implemented in the current version. They are planned for a future release. The VAR largely corrects inter-satellite calibration, except for small effects at boundaries between satellites. The satellite operators are responsible for detecting and eliminating navigation and telemetry errors.

.....

A number of \*known errors\* are contained in part or all of the current 3B42 archive. They have been uncovered by visual inspection and other diagnostics, but correction awaits the next reprocessing. Other items will be included in future re-processing cycles as possible. For ease of document maintenance, some of the following items imply the known error by stating what upgrade was applied.

- 1. AMSU-B estimates are deficient in sensing light precipitation, leading to an underestimate that is regionally dependent, but can approach 100% in light-rain areas. Because of this, the AMSU-B and MHS estimates are used only if no other HQ estimates are available, meaning that the deficiency is minimized in the TMPA. Nonetheless, it causes bias over oceans that begins in 2000 and fluctuates with the coverage by AMSU-B and MHS estimates.
- 2. GPROF estimates have a variety of artifacts associated with coastal regions that are sensorand scene-dependent. In particular, inland water bodies in the Southeastern U.S. (Tian and Peters-Lidard 2007), Lake Nasser in Egypt, and desert coastal regions show anomalous high precipitation, while oceanic coastal regions in a variety of rainy situations tend to be deficient in precipitation.

- 3. The GridSat-B1 inter-satellite calibration and zenith-angle correction schemes exhibit issues. In general this is not a problem due to the spatially varying microwave calibration. However, seams at satellite boundaries and differences when a given location alternates between two satellites are sometimes apparent.
- 4. SSMIS calibration and updates to the GPROF-SSMIS algorithm continue. The present solution for these issues is considered satisfactory, but not definitive.
- 5. The current satellite-gauge combination scheme allows coastal gauge data to "bleed" into coastal waters, up to 1° away from the coast. This is particularly noticeable where there is heavy precipitation in the gauge analysis, but modest values off-shore.
- 6. GOES-E data in the GridSat-B1 archive is highly noisy for 9-15 UTC 5 March 1998, 00Z March 25, and 21Z March 29, effectively preventing useful estimates over the Americas for IRprecipitation and precipitation. It is suggested to use HQprecipitation instead.

A number of \*known anomalies\* are documented and left intact at the discretion of the data producers.

- 1. The very first 3-hourly period (00 UTC on 1 January 1998) only has data for 0000-0130 UTC, lacking data from the end of 1997.
- 2. For the period 1 January 1998 29 February 2000, 10-km (subsampled), 3-hourly IR Tb data were used in the 3B42 processing ("GridSat-B1 IR Tb data set"). After 29 February 2000, the 4-km IR is used ("merged 4 km IR Tb data set"), which should provide a more accurate gridbox average.
- 3. For the period 1 January 1998 03 UTC 16 June 1998 there were no geo-IR data available in the Indian Ocean Sector. High-zenith-angle observations from adjacent satellites are used for fill-in as available.
- 4. GMS data in the GridSat-B1 archive are missing for 21 UTC 4 January 1998 21 UTC 8 January 1998. Since the Meteosat data over the Indian Ocean sector do not begin until mid-1998, this results in a lack of IR data (and holes in 3B42) over the East Asia sector.
- 5. The TRMM orbital altitude was raised from 350 to 401.5 km in August 2001 to extend the life of the mission by reducing the amount of fuel needed to maintain the orbit. This caused small changes in footprint size and minimum detectable precipitation rates. The Version 7 algorithms are supposed to account for these changes, but tests show small unavoidable differences that are still being researched.
- 6. The TRMM PR suffered an electronics failure on 29 May 2009. Data were lost until the "B-side" electronics were activated on 19 June 2009. Small residual differences remain between A-side and B-side data.
- 7. At 2045 UTC on 21 March 2012 GOES-15 (WEST) suffered a "bad momentum unload" and ceased recording data. Imaging was restored at 1722 UTC on 23 March 2012. In the interim GOES-13 (EAST) was shifted to recording full-disk images. Use of higher-zenith-angle GOES-13 and MTSat-1 data largely covers the gap caused by the GOES-15 drop-outs.
- 8. The mix of satellites has changed over time, which affects the overall performance of the algorithm in two ways. First, the relative weighting of conically scanning microwave imagers versus cross-track-scanning sounders shifts, and second, the relative proportion of IR-based estimates changes. The passive-microwave sensor inventory is shown in "sensors contributing to TMPA".

- 9. The V7 tropical-ocean average precipitation is consistently some 5% higher than the combined TMI-PR product (2B31) that serves as the calibrator (see "intercomparison results"). The basis for this difference is not explicated at this point, but the value is small enough and consistent enough that we chose to release the data as background work continues.
- 10. F17 SSMIS has anomalously high precip values for a few scans over Brazil in the 21Z 26 April 2013 3B42 HQ and multi-satellite precip fields.
- 11. A TRMM spacecraft anomaly resulted in the loss of most TRMM sensor data for the period 02-14 UTC on 12 November 2013, and additional issues resulted in data gaps during the period 20-23:30 UTC. This reduces the data content in 3B42/43 somewhat, but is not a serious issue overall.
- 12. Snow accumulation on the receiving antenna prevented reception of MTSAT-2 data from 1832 UTC on 14 February 2014 to 1232 UTC on 15 February 2014. The data are lost.
- 13. Metop-A experienced an anomaly that prevented data collection for 1400 UTC 27 March 2014–0746 UTC 21 May 2014.

# 10. Missing Value Estimation and Codes

There is generally no effort to *estimate missing values* in the single-source input data sets.	
All products in the TMPA use the *standard missing value* "-9999.9".	
All *missing hours* of a product result from completely absent input data for the given hour. the input file(s) is(are) available, the product file is created, even if it lacks any valid data.	If

## 11. Quality and Confidence Estimates

The \*accuracy\* of the precipitation products can be broken into systematic departures from the true answer (bias) and random fluctuations about the true answer (sampling), as discussed in Huffman (1997). The former are the biggest problem for climatological averages, since they will not average out. However, for short averaging periods the low number of samples and/or algorithmic inaccuracies tend to present a more serious problem for individual microwave data sets. That is, the sampling is spotty enough that the collection of values over, say, one day may not be representative of the true distribution of precipitation over the day. For VAR, the sampling is good, but the algorithm likely has substantial RMS error due to the weak physical connection between IR Tb's and precipitation.

Accordingly, the "random error" is assumed to be dominant, and estimates could be computed as discussed in Huffman (1997). Random error cannot be corrected.

The "bias error" is likely smaller, or at least contained. This is less true over land, where the lower-frequency microwave channels are not useful for precipitation estimation with our current state of knowledge. The state of the art at the monthly scale is reflected in the study by Smith et

al. (2006) and Adler et al. (2012). One study of the sub-monthly bias is provided by Tian et al. (2009).

.....

The TMPA \*intercomparison results\* continue to be developed. The time series of the global images shows good continuity in time and space. Overall, the analysis approach appears to be working as expected. See Huffman et al. (2007, 2010) for more information. Numerous studies by the community are listed in

ftp://precip.gsfc.nasa.gov/pub/trmmdocs/rt/TMPA citations.pdf.

Table 9 provides long-term (1998-2010) comparisons for the latitude band 30°N-S against several other data sets. The 100% water column provides information on the performance over open ocean. The 75% columns provide a typical land/ocean separation (working here at the 2.5° lat./long. scale). Note that all schemes are sensitive to the definition of "ocean", with the addition of near-coastal areas adding about 8% to the ocean total. In the following summary the proliferation of version numbers is necessary because it is precisely the upgrades implied by these version changes that drive the differences.

The differences over land and coast are largely driven by the change in the gauge analysis:

- 3B43 V6 was computed with the old GPCC Version 2 monitoring product for 1998-April 2005, and the NOAA/CPC CAMS analysis thereafter (for timeliness).
- 3B43 V7 uses the latest GPCC Version 4 Full analysis through 2010 and the GPCC Version 6 Monitoring analysis thereafter.
- CAMS turned out to have systematic differences from GPCC Version 2, usually lower, and both are low compared to the new GPCC analyses.
- Starting with Version 4, GPCC switched from analyzing gauge values to analyzing gauge anomaly values, then adding the anomalies to a high-resolution climatology. As well, GPCC has continued to amass additional data, improving both the climatology and the individual months.

The largest V7–V6 differences occur in mountainous regions, such as the Himalayan foothills, coastal Burma (Myanmar), Papua New Guinea, and northwestern South America. On the other hand, land values for 3B43 V7 and GPCP SG V2.2 are very close to each other because they use the same GPCC gauge analysis and because the gauge tends to dominate the land bias in most places. See the GPCC web site for more details on the gauge analyses.

The tropical ocean changes result from:

- The 3B43 V6 included deficient AMSU precipitation estimates for 2000-May 2007, particularly 2003-May 2007; in V7 the current AMSU algorithm is applied throughout.
- The calibrating satellite product (TRMM Combined Instrument, 2B31, which uses both TMI and PR) showed a modest increase from Version 6 to Version 7 of about 0.11 mm/d.
- The calibrated microwave data are some 3-5% higher than the 2B31 calibrator, for reasons not yet understood.

All three tended to cause more rainfall in the tropical oceans. On the whole, these tropical ocean increases are considered beneficial because 3B43 V6 validated low against the Pacific Ocean atoll rain gauges, and V7 data are much closer, although still somewhat low.

The land values for 3B43 V7 and GPCP SG V2.2 are very close to each other because they use the same GPCC gauge analysis and because the gauge tends to dominate the land bias in most places by construction. The increase in 3B43 land fromV6 to V7 results both from the shift to the new GPCC analysis, and the shift to using GPCC throughout, rather than employing CAMS after April 2005. For the first, GPCC shifted from using a SPHEREMAP analysis on the gauge values to creating the analysis on gauge anomalies, which are then added to a high-resolution climatology. As well, many additional stations have been added. For the second, the CAMS was used to get a timely product in V6, but experience showed that it tended to introduce a low bias.

Table 9. Averages for several precipitation data sets for the latitude band 30°N-S over the years 1998-2010, all in mm/d. Working on 2.5° lat./long. gridboxes, the first column is restricted to gridboxes with 100% water, representing open ocean, while the next two columns use a more typical land/ocean split at 75% water.

(mm/d)	100% water	75% water		
(11111/4)	ocean	ocean	land	total
3B43 V6	2.66	2.90	2.89	2.90
2B31 V7	2.86	3.08	2.94	3.04
3B43 V7	3.00	3.27	3.19	3.25
GPCP SG V2.2	2.79	3.01	3.16	3.05

Validation studies are being conducted under the auspices of the International Precipitation Working Group (IPWG) in Australia, the continental U.S., western Europe, parts of South America, and Japan (Ebert et al. 2007). Respectively, the web sites for these activities are:

http://cawcr.gov.au/projects/SatRainVal/validation-intercomparison.html

http://cics.umd.edu/~johnj/us web.html

http://meso-a.gsfc.nasa.gov/ipwg/ipwgeu home.html

http://cics.umd.edu/~dvila/web/SatRainVal/dailyval.html

http://www-ipwg.kugi.kyoto-u.ac.jp/IPWG/sat val Japan.html

Zhou et al. (2014) provide a creative "double mass" analysis showing how the time series of 3B42 and 3B42RT differ by location. It is possible that an extension of this approach would illuminate the changes introduced by the climatological calibration in October 2014.

.....

The \*diurnal cycle\* depicted in the 3-hourly 3B42 V7 (and all other versions) is affected by the particular mix of satellite sensors at any given time and place, in common with all other such satellite-based precipitation estimation systems. The diurnal cycle phase produced by IR estimates, which respond to cloud tops, is known to lag the phase of surface observations in many locations. The lag is highly variable, but frequently reported as up to 3 hours. The passive microwave estimates over land depend on the solid hydrometeors, which typically are confined

to the upper reaches of clouds. This dependence also leads to lags compared to surface observations, up to about 1.5 hours. Over ocean the passive microwave estimates are driven by the full vertical profile of precipitation for imagers, but primarily by solid hydrometeors for sounders. Thus, there is a mix of typical lags, minimal for imagers and up to 1.5 hours for sounders. When you consider the regional variability in the lags of the individual sensor types and the variable mix of sensors contributing to the diurnal cycle during different epochs of satellite coverage, the general statement is that lags are more likely early in the dataset, before many passive microwave satellites were available, and are more likely over land. The TRMM PR, being a radar, gives relatively unbiased estimates of the diurnal cycle, but its sampling is so sparse that it takes several years of data to allow a reasonable estimate to appear out of the sampling noise. See Kikuchi and Wang (2008), although their study with Version 6 will have larger lags due to concentrating early in the record and with fewer passive microwave satellites than Version 7 has for the bulk of their study period.

.....

The \*controlling factors on dataset performance\* critically depend on the calibration approach, since the time series of the completed data tend to follow the time series of the calibrator, at least on the large scale. All of the global precipitation data sets have some calibrating data source, which is necessary to control bias differences between contributing satellites. Otherwise, shifts in the contributing set of satellites at any given time can cause unphysical shifts in the behavior of the precipitation estimates. However, this calibration plays a large role in determining the interannual variation that the various data sets display. Experience shows that datasets/regions with passive microwave calibration (oceans for Global Precipitation Climatology Project [GPCP] monthly Satellite-Gauge [SG], and all regions for 3B42RT and the Integrated Multi-satellitE Retrievals for Global Precipitation Measurement [GPM] mission [IMERG] Early and Late) tend to have similar interannual fluctuations, while datasets/regions with combined passive/active microwave calibration (oceans for 3B42/43 and IMERG Final) tend to show a variation in the tropical oceans that leads the passive microwave-calibrated datasets by 3-6 months. Climatological calibrations might change the mean bias or even the seasonal cycle, but they should not change the interannual variations or long-term trends.

Analyses of monthly surface gauge data add another layer of calibration over land in some datasets. The combined precipitation research team at Goddard has major responsibility for the GPCP monthly SG combined product, the 3B43 monthly product, and the IMERG Final Run monthly product. In each case the multi-satellite data are averaged to the monthly scale and combined with the Global Precipitation Climatology Centre's (GPCC) monthly surface precipitation gauge analysis. In each case the multi-satellite data are adjusted to the large-area mean of the gauge analysis, where available (mostly over land), and then combined with the gauge analysis using a simple inverse estimated-random-error variance weighting. In all three data sets the gauge analysis has an important or dominant role in determining the final combined value for grid boxes in areas with "good" gauge coverage. [See Bolvin et al. (2009) for an example with GPCP.] Regions with poor gauge coverage, such as central Africa have a higher weight on the satellite input that has been corrected to the large-area bias of the gauges. The oceans are mostly devoid of gauges and therefore mostly lack such gauge input.

In contrast, the short-interval (as opposed to monthly, above) GPCP is the One-Degree Daily (1DD), the short-interval TMPA is 3B42 (3-hourly), and the short-interval IMERG (half-hourly). In each case the short-interval data are adjusted with a simple, spatially varying ratio to force the multi-satellite estimates to approximately average up to the corresponding monthly satellite-gauge product, with controls on the ratios to prevent unphysical results. Thus, monthly-average values of the short-interval data should be close to the average of the monthly datasets, which the developers consider more reliable than the short-interval datasets. In fact, compared to datasets that lack the adjustment to the monthly satellite-gauge estimates, the 1DD, 3B42, and IMERG Final half-hourly datasets tend to score better at timescales longer than a few days. This is presumably because the random error begins to cancel out as more samples are averaged together, leaving only the bias error. Of course, the short-interval datasets and regions that lack month-to-month surface gauge data input are more clearly driven by the behavior of the satellite input data.

.....

#### 12. Data Archives

The \*archive and distribution site\* for the official release of the TRMM Multi-Satellite Precipitation Analysis is:

Goddard Earth Sciences Data and Information Services Center NASA Goddard Space Flight Center Code 610.2

Greenbelt, MD 20771 USA Phone: +1-301-614-5224 Fax: +1-301-614-5268

Internet: help-disc@listserv.gsfc.nasa.gov

Web site: http://disc.gsfc.nasa.gov

Interactive Web-based access to the data and related fields is provided through Giovanni; see that topic for details.

Independent archive and distribution sites exist for the input data sets, and contact information may be obtained through G.J. Huffman (see "Documentation creator").

.....

\*DOIs for 3B42 and 3B43\* have been assigned using GPM-style naming. For completeness, this list also includes the TMPA-RT products and two value-added products computed at the GDISC that give daily accumulations.

Local file ID	DOI
TRMM_3B40RT_7	10.5067/TRMM/TMPA/3H-E-MW/7
TRMM_3B41RT_7	10.5067/TRMM/TMPA/3H-E-IR/7
TRMM_3B42RT_7	10.5067/TRMM/TMPA/3H-E/7
TRMM_3B42_7	10.5067/TRMM/TMPA/3H/7
TRMM 3B43 7	10.5067/TRMM/TMPA/MONTH/7

The full URL is https://doi.org/<DOI>.

.....

#### 13. Documentation

The \*documentation creator\* is:

Dr. George J. Huffman Code 612 NASA Goddard Space Flight Center Greenbelt, MD 20771 USA

> Phone: +1-301-614-6308 Fax: +1-301-614-5492

Internet: george.j.huffman@nasa.gov MAPL Precipitation Page: http://precip.gsfc.nasa.gov/

.....

## The \*documentation revision history\* is:

22 October 2007	Version 1	by GJH, DTB
28 December 2007	Rev. 1.1	by GJH
26 February 2008	Rev. 1.2	by GJH
08 September 2009	Rev. 1.3	by GJH
15 April 2010	Rev. 1.4	by GJH
24 May 2010	Rev. 1.5	by GJH
16 February 2010	Rev. 1.6	by GJH
28 April 2011	Rev. 1.7	by GJH
22 May 2012	Version 2	by GJH
28 January 2013	Rev. 2.1	by GJH
15 February 2014	Rev. 2.2	by GJH
25 May 2014	Rev. 2.3	by GJH
3 July 2014	Rev. 2.4	by GJH; Add diurnal cycle
8 April 2015	Rev. 2.5	by GJH; end of mission content
19 April 2017	Rev. 2.6	by GJH; refresh links, Giovanni
28 June 2017	Rev. 2.7	by GJH; 2A12 thresholding
26 April 2018	Rev. 2.7	by GJH; DOIs; IMERG timing

The list of \*references\* used in this documentation is:

Adler, R.F., G. Gu, G.J. Huffman, 2012: Estimating Climatological Bias Errors for the Global Precipitation Climatology Project (GPCP). *J. Appl. Meteor. and Climatol.*, **51**(1), doi:10.1175/JAMC-D-11-052.1, 84-99.

- Andersson, A., K. Fennig, C. Klepp, S. Bakan, H. Graßl, J. Schulz, 2010: The Hamburg Ocean Atmosphere Parameters and Fluxes from Satellite Data HOAPS-3. *Earth Syst. Sci. Data*, **2**, 215-234, doi:10.5194/essd-2-215-2010.
- Bolvin, D.T., R.F. Adler, G.J. Huffman, E.J. Nelkin, J.P. Poutiainen, 2009: Comparison of GPCP Monthly and Daily Precipitation Estimates with High-Latitude Gauge Observations. *J. Appl. Meteor. Climatol.*, **48**, 1843–1857.
- Ebert, E.E., J.E. Janowiak, C. Kidd, 2007: Comparison of Near-Real-Time Precipitation Estimates from Satellite Observations and Numerical Models. *Bull. Amer. Meteor. Soc.*, **88**(1), 47-64.
- Chiu, L.S., R. Chokngamwong, 2010: Microwave Emission Brightness Temperature Histograms (METH) Rain Rates for Climate Studies: Remote Sensing Systems SSM/I Version-6 Results. *J.Appl. Met. Clim.*, **49**, 115-123.
- Grody, N.C., 1991: Classification of Snow Cover and Precipitation Using the Special Sensor Microwave/Imager (SSMI). *J. Geophys. Res.*, **96**, 7423-7435.
- Haddad, Z.S., D.A. Short, S.L. Durden, E. Im, S. Hensley, M.B. Grable, R.A. Black, 1997a: A New Parameterization of the Rain Drop Size Distribution. *IEEE Trans. Geosci. Remote Sens.*, **35**, 532-539.
- Haddad, Z.S., E.A. Smith, C.D. Kummerow, T. Iguchi, M.R. Farrar, S.L. Durden, M. Alves, W.S. Olson, 1997b: The TRMM "Day-1" Radar/Radiometer Combined Rain-Profiling Algorithm. *J. Meteor. Soc. Japan*, **75**, 799-809.
- Hollinger, J., R. Lo, G. Poe, J. Pierce, 1987: *Special Sensor Microwave/Imager User's Guide*, Naval Res. Lab., Washington, DC.
- Hollinger, J.P., J.L. Pierce, G.A. Poe, 1990: SSMI Instrument Evaluation. *IEEE Trans. Geosci. Remote Sens.*, **28**, 781-790.
- Huffman, G.J., 1997: Estimates of Root-Mean-Square Random Error Contained in Finite Sets of Estimated Precipitation. *J. Appl. Meteor.*, **36**, 1191-1201.
- Huffman, G.J., R.F. Adler, D.T. Bolvin, G. Gu, E.J. Nelkin, K.P. Bowman, Y. Hong, E.F. Stocker, D.B. Wolff, 2007: The TRMM Multi-satellite Precipitation Analysis: Quasi-Global, Multi-Year, Combined-Sensor Precipitation Estimates at Fine Scale. *J. Hydrometeor.*, **8**(1), 38-55. PDF available at *ftp://meso.gsfc.nasa.gov/agnes/huffman/papers/TMPA\_jhm\_07.pdf.gz*
- Huffman, G.J., R.F. Adler, D.T. Bolvin, E.J. Nelkin, 2010: The TRMM Multi-satellite Precipitation Analysis (TMPA). Chapter 1 in *Satellite Rainfall Applications for Surface Hydrology*, F. Hossain and M. Gebremichael, Eds. Springer Verlag, ISBN: 978-90-481-2914-0, 3-22.
- Huffman, G.J., R.F. Adler, S. Curtis, D.T. Bolvin, E.J. Nelkin, 2007: Global Rainfall Analyses at Monthly and 3-hr Time Scales. Chapter 23 of *Measuring Precipitation from Space: EURAINSAT and the Future*, V. Levizzani, P. Bauer, and F.J. Turk, Eds., Springer Verlag (Kluwer Academic Pub. B.V.), Dordrecht, The Netherlands, 291-306. [Invited paper]
- Huffman, G.J., R.F. Adler, E.F. Stocker, D.T. Bolvin, E.J. Nelkin, 2003: Analysis of TRMM 3-Hourly Multi-Satellite Precipitation Estimates Computed in Both Real and Post-Real Time. *Combined Preprints CD-ROM*, 83rd AMS Annual Meeting. Paper P4.11 in 12th Conf. on Sat. Meteor. and Oceanog., 9-13 Feb. 2003, Long Beach, CA, 6 pp.
- Huffman, G.J., D.T. Bolvin, 2015: Transition of 3B42/3B43 Research Product from Monthly to Climatological Calibration/Adjustment. http://pmm.nasa.gov/sites/default/files/document\_files/3B42\_3B43\_TMPA\_restart.pdf, 11 pp.

40

- Huffman, G.J., D.T. Bolvin, D. Braithwaite, K. Hsu, R. Joyce, C. Kidd, E.J. Nelkin, S. Sorooshian, J. Tan, P. Xie, 2018: Algorithm Theoretical Basis Document (ATBD) Version 5.2 for the NASA Global Precipitation Measurement (GPM) Integrated Multi-satellitE Retrievals for GPM (I-MERG). GPM Project, Greenbelt, MD, 35 pp. https://pmm.nasa.gov/sites/default/files/document\_files/IMERG\_ATBD\_V5.2.pdf
- Janowiak, J.E., P.A. Arkin, 1991: Rainfall Variations in the Tropics during 1986-1989. *J. Geophys. Res.*, **96**, 3359-3373.
- Joyce, R.J., J.E. Janowiak, P.A. Arkin, P. Xie, 2004: CMORPH: A Method that Produces Global Precipitation Estimates from Passive Microwave and Infrared Data at 8 Km, Hourly Resolution. *J. Climate*, **5**, 487-503.
- Joyce, R.J., J.E. Janowiak, G.J. Huffman, 2001: Latitudinal and Seasonal Dependent Zenith Angle Corrections for Geostationary Satellite IR Brightness Temperatures. *J. Appl. Meteor.*, **40**(4), 689-703.
- Kikuchi, K., B. Wang, 2008: Diurnal Precipitation Regimes in the Global Tropics. *J. Climate*, **21**, doi:10.1175/2007JCLI2051.1, 2680-2696.
- Kongoli, C., P. Pellegrino, R. Ferraro, 2007: The Utilization of the AMSU High Frequency Measurements for Improved Coastal Rain Retrievals. *Geophys. Res. Lett.*, **34**, L17809, doi:10.1029/2007GL029940.
- Kubota T., S. Shige, H. Hashizume, K. Aonashi, N. Takahashi, S. Seto, M. Hirose, Y.N. Takayabu, K. Nakagawa, K. Iwanami, T. Ushio, M. Kachi, K. Okamoto, 2007: Global Precipitation Map Using Satellite-Borne Microwave Radiometers by the GSMaP Project: Production and Validation. *IEEE Trans. Geosci. Remote Sens.*, **45**, 2259-2275.
- Kummerow, C., Y. Hong, W.S. Olson, S. Yang, R.F. Adler, J. McCollum, R. Ferraro, G. Petty, D-B. Shin, T.T. Wilheit, 2001: The Evolution of the Goddard Profiling Algorithm (GPROF) for Rainfall Estimation from Passive Microwave Sensors. *J. Appl. Meteor.*, **40**, doi:/10.1175/1520-0450(2001)040<1801:TEOTGP>2.0.CO;2, 1801–1820.
- Kummerow, C., W.S. Olson, L. Giglio, 1996: A Simplified Scheme for Obtaining Precipitation and Vertical Hydrometeor Profiles from Passive Microwave Sensors. *IEEE Trans. Geosci. Remote Sens.*, **34**, 1213-1232.
- Kummerow, C., W. Barnes, T. Kozu, J. Shiue, J. Simpson, 1998: The Tropical Rainfall Measuring Mission (TRMM) Sensor Package. *J. Atmos. Oceanic Tech.*, **15**(3), 809-817.
- Legates, D.R, 1987: A Climatology of Global Precipitation. *Pub. in Climatol.*, **40**, U. of Delaware.
- Northrup Grumman, 2002: Algorithm and Data User Manual (ADUM) for the Special Sensor Microwave Imager/Sounder (SSMIS). Northrup Grumman Electronic Systems, Azusa, CA, Report 12621, 69 pp. ftp://rain.atmos.colostate.edu/pub/msapiano/SSMI\_SSMIS\_Archive\_Docs/SSMIS\_general/Algorithm\_and\_Data\_User\_Manual\_For\_SSMIS\_Jul02.pdf
- Olson, W. S., C. D. Kummerow, Y. Hong, W.-K. Tao, 1999: Atmospheric Latent Heating Distributions in the Tropics Derived from Satellite Passive Microwave Radiometer Measurements. *J. Appl. Meteor.*, **38**, 633-664.
- Parsons, M.A., R. Duerr, J.-B. Minster, 2010: Data Citation and Peer Review. EOS, 91(34), 297-298.
- PMM, 2014: Goodbye to TRMM, First Rain Radar in Space. http://pmm.gsfc.nasa.gov/articles/goodbye-trmm-first-rain-radar-space
- Rudolf, B., 1993: Management and Analysis of Precipitation Data on a Routine Basis. *Proceedings of International Symposium on Precipitation and Evaporation*, Vol. 1, B. Sevruk and M. Lapin, Eds., Slovak Hydrometeorology Institution, 69-76.

- Schneider, U., A. Becker, A. Meyer-Christoffer, M. Ziese, B. Rudolf, 2010: Global Precipitation Analysis Products of the GPCC. Global Precipitation Climatology Centre, DWD, 12 pp. Available on-line at http://www.dwd.de/as GPCC intr products 2008.pdf.
- Smith, T.M., P.A. Arkin, J.J. Bates, G.J. Huffman, 2006: Estimating Bias of Satellite-Based Precipitation Estimates. *J. Hydrometeor.*, 7(5), 841-856.
- Sorooshian, S., K.-L. Hsu, X. Gao, H.V. Gupta, B. Imam, D. Braithwaite 2000: Evaluation of PERSIANN System Satellite-Based Estimates of Tropical Rainfall. *Bull. Amer. Meteor. Soc.*, **81**, 2035-2046.
- Spencer, R.W., 1993: Global Oceanic Precipitation from the MSU During 1979-92 and Comparisons to Other Climatologies. *J. Climate*, **6**, 1301-1326.
- Tian, Y., C.D. Peters-Lidard, 2007: Systematic Anomalies over Inland Water Bodies in Satellite-Based Precipitation Estimates. *Geophys. Res. Lett.*, **34**, doi:1029/2007GL030787.
- Turk, F.J., G.D. Rohaly, J. Hawkins, E.A. Smith, F.S. Marzano, A. Mugnai, V. Levizzani, 1999: Meteorological Applications of Precipitation Estimation from Combined SSMI, TRMM and Infrared Geostationary Satellite Data. *Microwave Radiometry and Remote Sensing of the Earth's Surface and Atmosphere*, P. Pampaloni and S. Paloscia Eds., VSP Int. Sci. Publ., 353-363.
- Vila, D., R. Ferraro, R. Joyce, 2007: Evaluation and Improvement of AMSU Precipitation Retrievals. *J. Geophys. Res.*, **112**, D20119, doi:10.1029/2007JD008617.
- Vila, D., C. Hernandez, R. Ferraro, H. Semunegus, 2013: The Performance of Hydrological Monthly Products Using SSM/I SSMI/S Sensors. *J. Hydrometeor.*, **14**, doi:10.1175/JHM-D-12-056.1, 266-274.
- Villarini, G., W.F. Krajewski, 2007: Evaluation of the Research-Version TMPA Three-Hourly 0.25°x0.25° Rainfall Estimates over Oklahoma. *Geopys. Res. Lett.*, **34**, doi:10.1029/2006GL029147.
- Weng, F., L. Zhao, R. Ferraro, G. Poe, X. Li, N. Grody, 2003: Advanced Microwave Sounding Unit Cloud and Precipitation Algorithms. *Radio Sci.*, **38**, 8068-8079.
- Wentz, F.J., and R.W. Spencer, 1998: SSMI Rain Retrievals within a Unified All-Weather Ocean Algorithm. *J. Atmos. Sci.*, **55**(9), 1613-1627.
- Wilheit, T., A. Chang, L. Chiu, 1991: Retrieval of Monthly Rainfall Indices from Microwave Radiometric Measurements Using Probability Distribution Function. *J. Atmos. Ocean. Tech.*, **8**, 118-136.
- Willmott, C.J., C.M. Rowe, W.D. Philpot, 1985: Small-Scale Climate Maps: A Sensitivity Analysis of Some Common Assumptions Associated with Grid-Point Interpolation and Contouring. *Amer. Cartographer*, **12**, 5-16.
- Yong, B., B. Chen, Y. Hong, J.J. Gourley, Z. Li, 2015: Impact of Missing Passive Microwave Sensors on Multi-Satellite Precipitation Retrieval Algorithm. *Rem. Sens.*, in review.
- Zhao, L., F. Weng, 2002: Retrieval of Ice Cloud Parameters Using the Advanced Microwave Sounding Unit. *J. Appl. Meteor.*, **41**, 384-395.
- Zhou, T., B. Nijssen, G.J. Huffman, D.P. Lettenmaier, 2014: Evaluation of the TRMM Real-Time Multi-Satellite Precipitation Analysis Version 7 for Macroscale Hydrologic Prediction. *J. Hydrometeor.*, **15**(4), 1651–1660. *doi: http://dx.doi.org/10.1175/JHM-D-13-0128.1*.

Web Sites:

AMS data citation policy: http://www2.ametsoc.org/ams/index.cfm/publications/authors/journal-and-bams-authors/journal-and-bams-authors-guide/data-archiving-and-citation/

AMSR instrument: http://www.ghcc.msfc.nasa.gov/AMSR/

AMSU-B instrument: http://www2.ncdc.noaa.gov/docs/klm/html/c3/sec3-4.htm in the NOAA KLM User's Guide (September 2000 revision):

http://www2.ncdc.noaa.gov/docs/klm/index.htm

Giovanni: https://giovanni.sci.gsfc.nasa.gov/giovanni/

IMERG ATBD: https://pmm.nasa.gov/sites/default/files/document\_files/IMERG\_ATBD\_V5.2.pdf IPWG Validation for Australia: http://cawcr.gov.au/projects/SatRainVal/validation-intercomparison.html

IPWG Validation for U.S.: http://cics.umd.edu/~johnj/us\_web.html

IPWG Validation for western Europe: http://meso-a.gsfc.nasa.gov/ipwg/ipwgeu\_home.html

IPWG Validation for South America: http://cics.umd.edu/~dvila/web/SatRainVal/dailyval.html

IPWG Validation for Japan: http://www-ipwg.kugi.kyoto-u.ac.jp/IPWG/sat\_val\_Japan.html

MAPL Precipitation Page: http://precip.gsfc.nasa.gov/

MHS instrument: http://www2.ncdc.noaa.gov/docs/klm/html/c3/sec3-9.htm in the NOAA KLM User's Guide (September 2000 revision):

http://www2.ncdc.noaa.gov/docs/klm/index.htm

PPS home: http://pps.gsfc.nasa.gov

Satellite overpass times: http://precip.gsfc.nasa.gov/times\_allsat.jpg

TMPA data: http://trmm.gsfc.nasa.gov/data\_dir/data.html

TMPA data format and toolkit: http://pps.gsfc.nasa.gov/tsdis/Documents/Tutorial.pdf TMPA paper: ftp://meso.gsfc.nasa.gov/agnes/huffman/papers/TMPA jhm 07.pdf.gz

TRMM home: http://trmm.gsfc.nasa.gov/

\*Acronyms\*

ASCII American Standard Code for Information Interchange (i.e., text)

AIRS Atmospheric Infrared Sounder

AMSR-E Advanced Microwave Scanning Radiometer for Earth Observing System

AMSU Advanced Microwave Sounding Unit
ATBD Algorithm Theoretical Basis Document
AVHRR Advanced Very High Resolution Radiometer

CMORPH CPC MORPHing algorithm

CMORPH-KF Kalman Filter version of CMORPH

CPC Climate Prediction Center

CPU Central Processing Unit (of a computer)

CSU Colorado State University dBZ decibels of reflectivity factor De particle effective diameter size

DISC Data and Information Services Center
DMSP Defense Meteorological Satellite Program

DOI Digital Object Identifier

ESSIC (University of Maryland College Park) Earth System Science Interdisciplinary

Center

EUMETSAT EUropean organization for the exploitation of Meteorological Satellites

FA Fraction of Ambiguous

FNMOC Fleet Numerical Meteorological and Oceanographic Center

FTP File Transfer Protocol

GDAS Global Data Assimilation System

GES Goddard Earth Sciences

GHRC Global Hydrological Research Center

GHz Gigahertz

GIS Geographical Information System

GMS Geosynchronous Meteorological Satellite

GOES Geosynchronous Operational Environmental Satellites

GPCC Global Precipitation Climatology Centre GPM Global Precipitation Measurement mission

GPROF Goddard Profiling algorithm
GridSat-B1 Gridded Satellite data – B1
GSFC Goddard Space Flight Center

GSMaP Global Satellite Map of Precipitation

HDF Hierarchical Data Format

HQ High Quality (microwave precipitation)

IDL Interactive Data Language

IMERG Integrated Multi-satellitE Retrievals for GPM IPWG International Precipitation Working Group

IR Infrared

ISCCP International Satellite Cloud Climatology Project

IWP Ice Water Path

JAXA Japanese Aerospace Exploration Agency

KB Kilobytes

lat/lon latitude/longitude LEO Low Earth orbit

MAPL Mesoscale Atmospheric Processes Laboratory

MB megabytes

Meteorological Satellite

MetOp Operational Meteorological satellite
MHS Microwave Humidity Sounder

MM5 NCAR/PSU Mesoscale Model Version 5

MSFC Marshall Space Flight Center

MSPPS Microwave Surface and Precipitation Products System

MSU Microwave Sounding Unit

MTSat Multifunctional Transport Satellite

NASA National Aeronautics and Space Administration NCAR National Center for Atmospheric Research

NCDC National Climatic Data Center

NESDIS National Environmental Satellite Data and Information Service

NOAA National Oceanic and Atmospheric Administration

NSIDC National Snow and Ice Data Center

NWS National Weather Service

PERSIANN Precipitation Estimation from Remotely Sensed Information using Artificial

**Neural Networks** 

PERSIANN-CCS

PERSIANN with Cloud Classification System

PPS Precipitation Processing System
PR (TRMM) Precipitation Radar
PSU Pennsylvania State University

RT Real Time

SDR Satellite Data Record SG Satellite-Gauge

SSMI Special Sensor Microwave/Imager

SSMIS Special Sensor Microwave Imager-Sounder SSM/T2 Special Sensor Microwave/Temperature 2

Ta Antenna Temperature
Tb Brightness Temperature

TCI TRMM Combined Instrument algorithm (2B31)

TMI TRMM Microwave Imager

TMPA TRMM Multi-satellite Precipitation Algorithm

TMPA-RT Real-Time TMPA

TRMM Tropical Rainfall Measuring Mission

URL Universal Resource Location

UTC Universal Coordinated Time (same as GMT, Z)

VAR VAriable Rainrate (IR precipitation)

V6 Version 6 V7 Version 7

Zo Surface reflectivity

.....

A \*Frequently Asked Questions (FAQ)\* list is being assembled and maintained by the Goddard Earth Science Data and Information Services Center (GESDISC). It is posted at: http://disc.sci.gsfc.nasa.gov/additional/faq/precipitation\_faq.shtml.

.....

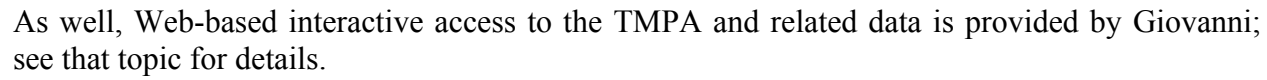
### 14. Inventories

The \*data set inventory\* may be obtained by accessing the 3B42 and 3B43 product listings at https://pmm.nasa.gov/data-access/pps-ftp#arthurhou-trmmdata/ or by contacting the representative listed in section 12.

.....

### 15. How to Order Data and Obtain Information about the Data

Users interested in \*obtaining data\* should access the 3B42 and 3B43 product listings at https://pmm.nasa.gov/data-access/pps-ftp#arthurhou-trmmdata/ or by contacting the representative listed in section 12.



The \*data access policy\* is "freely available" with three common-sense caveats:

1. It is an emerging best practice that the data set source should be referenced when the data are used. Current TMPA data sets have not been given DOI's. A formal reference of the form

Huffman, G.J., E.F. Stocker, D.T. Bolvin, E.J. Nelkin, 2014, last updated 2014: <*dataset identifier> Data Sets.* NASA/GSFC, Greenbelt, MD, USA, <dataset archive *URL>*.

where <dataset archive URL> is now given by the DOI (see "DOIs for 3B42 and 3B43"), is suggested following the AMS policy statement at

http://www2.ametsoc.org/ams/index.cfm/publications/authors/journal-and-bams-authors/journal-and-bams-authors-guide/data-archiving-and-citation/.

Note that the AMS policy states that this dataset reference should be in addition to reference to the relevant papers on constructing the data set. This approach allows readers to find both the technical literature and the data archive.

- 2. New users should obtain their own current, clean copy, rather than taking a version from a third party that might be damaged or out of date.
- 3. Errors and difficulties in the dataset should be reported to the dataset creators.

.....